OULUN YLIOPISTO

FACULTY OF INFORMATION TECHNOLOGY AND ELECTRICAL ENGINEERING

DEGREE PROGRAMME IN ELECTRONICS AND COMMUNICATIONS ENGINEERING

MASTER'S THESIS

RELIABILITY TESTING ON STRETCHABLE ELECTRONICS – PRINTED CONDUCTORS UNDER STRAIN

Author	Arttu Korhonen
Supervisor	Tapio Fabritius
Second Examiner	Christian Schuss
Technical Advisor	Tuomas Happonen

March 2019

Korhonen A. (2019) Reliability testing on stretchable electronics – printed conductors under strain. University of Oulu, Faculty of Information Technology and Electrical Engineering, Degree Programme in Electronics and Communications Engineering, Master's Thesis, 71 p.

ABSTRACT

The aim of stretchable electronics research is to develop stretchable circuit boards and devices that can replace today's hard and rigid circuit boards and devices. Stretching would allow for more comfortable, flexible and stretchable devices.

The aim of this thesis is to investigate the properties of printed conductors on a stretched substrate, the requirements for testing, and to produce a device for stretch testing which meets desired requirements. The properties of the printed conductor are influenced by the used fabrication technique and the drying times, as well as materials such as printing ink and substrate. The properties affect the reliability and durability of the conductor, for example, failure mechanisms such as cracking and delamination of the conductor.

Requirements for the test device is 1 % accuracy as a standard for the measuring instrument, which was achieved for the measuring instruments in this thesis. With the test apparatus implemented in the thesis, the stretchability limit test was performed on samples made using silk screen printing. The samples used five different printing inks, six drying times, three substrate thicknesses, four wire patterns and horizontal and vertical printing directions. The best wire pattern for the stretchability limit test was the U-shaped conductor. The horizontal printing direction was better than the vertical and the thickest 150 µm substrate was better than thinner ones.

The second cyclic stretchability test performed by the test device was performed on samples with the evenly performed ink in the stretchability limit test. The measurement was performed on ten identical samples giving very similar results, which were made using the roll-to-roll technique. Based on the first test, the samples were horizontally printed on a 150 µm substrate, and the wire was U-shaped. All samples failed between 111–168 cycles when limit of failure was 100 Ω average resistance per cycle. Based on the Weibull distribution of the results, 63.2 % of the tested samples failed at cycle 149.

Key words: printed electronics, silk screen printing, stretchability limit test, cyclic stretchability test, Weibull distribution.

Korhonen A. (2019) Venyvän elektroniikan luotettavuustestausta – painetut johtimet venytyksessä. Oulun yliopisto, tieto- ja sähkötekniikan tiedekunta, elektroniikan ja tietoliikennetekniikan tutkinto-ohjelma. Diplomityö, 71 s.

TIIVISTELMÄ

Venyvän elektroniikan tutkimuksen tavoitteena on kehittää venyviä alustoja ja venyviä laitteita, joilla voidaan korvata kovia ja kiinteitä nykypäivän piirilevyjä ja laitteita. Venyvyys mahdollistaisi mukavampien, taipuisien ja venyvien laitteiden valmistamisen.

Tämän tutkielman tavoitteena on perehtyä venyvälle substraatille painetun johtimen ominaisuuksiin, testauksen vaatimuksiin ja toteuttaa vaatimusten mukainen laite venytystestaukseen. Painetun johtimen ominaisuuksiin vaikuttavat käytetyt valmistusmenetelmät ja kuivausajat sekä materiaalit kuten painomuste ja substraatti. Ominaisuudet vaikuttavat johtimen luotettavuuteen ja kestävyyteen, esimerkiksi vikaantumismekanismeihin, kuten johtimen halkeiluun ja delaminoitumiseen.

Testilaitteen vaatimuksena käytetään standardeissa mittalaitteille vaadittua 1 % tarkkuutta, minkä tutkielmassa toteutettu mittalaite täyttää kaikilta osin. Tutkielmassa toteutetulla testilaitteella suoritettiin maksimivenymän testi tasosilkillä valmistetulle näytteille. Näytteissä käytettiin viittä eri painomustetta, kuutta kuivausaikaa, kolmea substraatin paksuutta, neljää johdinkuviota, sekä horisontaalista että vertikaalista painosuuntaa. Painokuvioista parhaiten maksimivenymän testissä kesti U-muotoinen johdin, horisontaalinen painosuunta oli vertikaalista parempi ja paksuin 150 µm substraatti ohuempia parempi.

Testilaitteella toteutettu toinen syklisen venytyksen kesto mittaus suoritettiin maksimivenymän testissä tasaisimmin suoriutuneelle musteelle. Mittaus suoritettiin kymmenelle identtiselle roll-to-roll menetelmällä valmistetulle näytteelle, joista saatiin hyvin tasaiset tulokset. Näytteet olivat ensimmäisen testin perusteella horisontaalisesti 150 µm substraatille painettuja ja johdin oli U-muotoinen. Kaikki näytteet vikaantuivat 111-168 syklien välissä, kun vikaantumisen määritelmä oli syklin keskimääräisen resistanssin ylittäminen 100 Ω raja-arvon. Tuloksista muodostetun Weibullin jakauman perusteella testatun kaltaisista näytteistä 63,2 prosenttia on vikaantunut 149 syklin kohdalla.

Avainsanat: painettava elektroniikka, silkkipaino, maksimivenymän testi, syklisen venytyksen kesto testi, Weibullin jakauma.

TABLE OF CONTENTS

FOREWORD

This thesis was carried out in VTT Oulu, during the end of October 2018 to March 2019. The purpose of the thesis was to introduce a stretching device for printed conductors of stretchable electronics, and to make measurements on the device at the beginning of the ELASTRONICS project.

I would like to thank my research team leader, Teemu Alajoki, for his confidence and the opportunity to carry out this thesis on the flexible electronics integration team. I would also like to thank the technical adviser, Tuomas Happonen, and everyone who has participated in the work of the thesis. Special thanks to supervisor Tapio Fabritius for good guidance and advice, and thanks to second examiner, Christian Schuss.

Finally, I would like to thank my parents, my wife and family, my siblings and friends for their support and interest in my thesis.

Oulu, March 14, 2019

Arttu Korhonen

LIST OF SYMBOLS AND ABBREVIATIONS

a	Thread spacing
A_λ	Amplitude of a modulation
c	Confidence level
d	Thread thickness
E	Surface energy of material
$E_{1,2}$	Surface energy of material
E_{12}	Surface energy of materials interface
h	Film thickness
h_o	Mean value of the printed layer
h_1	Amplitude of the printed layer surface
i,j	Unit vectors
n	Sample size
n_0	Minimum sample size
p_L	Laplace pressure
r	Radius of liquid drop
R	Resistance
R_0	Initial resistance, resistance starting value
R_s	Reliability level
s	Standard deviation
t	Time
$v_{i,j}$	Fluid's flow velocity
v_p	Printing speed
w	Mesh width
W_{adh}	Work of adhesion
W_{coh}	Work of cohesion
$W_{LS}^{(adh)}$	Energy of adhesion
x	Direction
$x_{i,j}$	Distance which liquid travelled
$\bar{X}$	Point estimate, i.e. mean value of samples
y	Parameter of the failure rate and the cumulative distribution function, example time or number of cycles
z	Standard normal distribution value for confidence level
A_i	Area
F_j	Force

COM	Communication port
DOD	Drop on demand inkjet
ECG	Electrocardiography, electrical activity of the heart
EMG	Electromyography, electrical activity of muscles
LED	Light emitting diode
PC	Personal computer

PDMS	Polydimethylsiloxane
PET	Polyethylene terephthalate
TPU	Thermoplastic polyurethane
UV	Ultraviolet
VTT	VTT Technical Research Centre of Finland Ltd

∂	Derivate
α	Scale parameter
α_s	Exponent which describe shear thickness
β	Shape parameter
Υ_{SL}	The surface energy (tension) of the liquid-solid interface
γ	Shear rate
$\gamma_{i,j,k}$	Shear rate in unit vector
ϵ	Strain rate at percent unit
η	Dynamic viscosity
θ	Contact angle
λ	Wavelength
λ_{vf}	Viscous fingering wavelength
π	Pi
σ	Surface tension
σ_{LG}	Surface tension (liquid-gas interface)
σ_{SG}	Surface tension (surface-gas interface)
σ_{SL}	Surface tension (surface-liquid interface)
τ	Shear stress
τ_{ij}	Shear stress
τ_{λ}^{rel}	Relaxation in timescale
τ_{vf}^{rel}	Viscous fingering in timescale
τ_{λ}^{m}	Marangoni in timescale
Δ	A change of quantity

1 INTRODUCTION

Traditional electric circuits have rigid, inflexible and un-stretchable silicon-based structures and circuit boards that are very difficult to adjust for user-friendly wearable devices. Due to the rigid component structures, modules and devices will also be rigid, making them non-optimal for wearables. By exploiting novel stretchable materials and fabrication techniques, more comfortable, stretchable and flexible devices for measuring heart rate and ECG, for example, can be made. Stretchable structures and material make it possible to incorporate user-friendly devices into clothes. Successful outcomes from these efforts have the potential to change our conception of electronics, from hard, rigid, planar chips to soft, stretchable, curvilinear sheets [1]. At their best, these devices can even form an invisible part of our clothes, allowing health monitoring via sensors without a need for separate equipment.

At present, there is a small number of stretchable electronics devices that are available to consumers. Their price levels are still very high, and they are not fully stretchable, but also contain traditional hard modules. These devices also have some problems related to resistance to washing. Before these traditional modules can be changed into soft, washable and stretchable parts of devices, reducing the price level and making products available to all consumers, there are several challenges to be overcome. There are challenges in term of materials, fabrication techniques, and components as well as testing. Wearable electronics application devices and materials should be as soft and as stretchable as human skin [2]. The manufacture of stretchable electronics should utilize cost-effective manufacturing methods that can produce large quantities of ready circuits. The components of stretchable electronics should be tiny, flexible and preferably stretchable, and the connection between components and a stretchy substrate must be reliable. For effective testing, reliable ways to test stretchy components and devices need to be developed. Testing should respond as well as possible to a product's end-use environment and the stresses within the environment. This will ensure that the device is durable and reliable for its intended use. However, one of the biggest challenges of stretchable electronics is that mechanical and electrical functionality must be preserved under all strain values [3].

This thesis focuses on investigating problems associated with the testing of stretchable electronics and working out the testing problem of substrates and conductors. Stretchable, reliable and high-performance substrates and conductors provide a stable foundation for stretchable electronic devices. The samples used in this thesis are produced by printing, because printing is a cost-effective and fast way to produce a large number of samples. This enables a fast transition from sample production to finished device production at a later stage.

VTT Technical Research Centre of Finland Ltd.'s Oulu office does not yet have a device for testing the strain of samples. Suitable test equipment will be introduced later in the thesis. The test equipment gives information on the force and distance of stretching and these parameters can be compared together. In addition, resistance measurement is coupled to the testing equipment so that resistance changes can be followed during stretching in order to compare this with the distance and the force.

The structure of this thesis is as follows: Chapter 2 examines stretchable electronics and their history. In addition, this chapter explores the possibilities of stretchable electronics applications, stretchable electronics materials, and fabrication techniques. Chapter 3 deals with reliability in general, and why reliability testing is done. The chapter also examines standards of stretchable electronics and the ways in which major organizations test stretchable electronics. Chapter 4 examines the test device, setups and measurements. The measurement results are also presented. Chapter 5 discusses the reliability of the test device and critically

examines the measurement results. Finally, Chapter 6 summarizes the thesis, going through the objectives, reviewing the main points of the thesis and briefly reviewing the results achieved.

2 STRETCHABLE ELECTRONICS

This chapter deals with stretchable electronics on a general level, briefly discussing what stretchable electronics are and their history. In addition, the possibilities and challenges of stretchable electronics as well as different fabrication techniques and materials are considered.

2.1 Stretchable electronics

Stretchable electronics is a very broad term. In practice it refers to all electric materials, components, devices and systems that exhibit some degree of mechanical stretchability and flexibility [4]. More specifically, it is an emerging class of electronics based on building electronic circuits and devices on stretchable substrates [3]. In some contexts, stretchable electronics are also referred to as elastic electronics.

There are numerous applications for stretchable electronics. The implementation depends on the used materials, the desired stretchability and the application. Roughly speaking, ways of implementing stretchable electronics can be divided into two main categories: conductivity stretchable applications, which are implemented mainly on a structure, and stretchable applications, which are affected materials such as stretching ink or fluid. A breakdown of stretchable electronics by conductive structure is shown in Figure 1 [1, 3, 5-8].

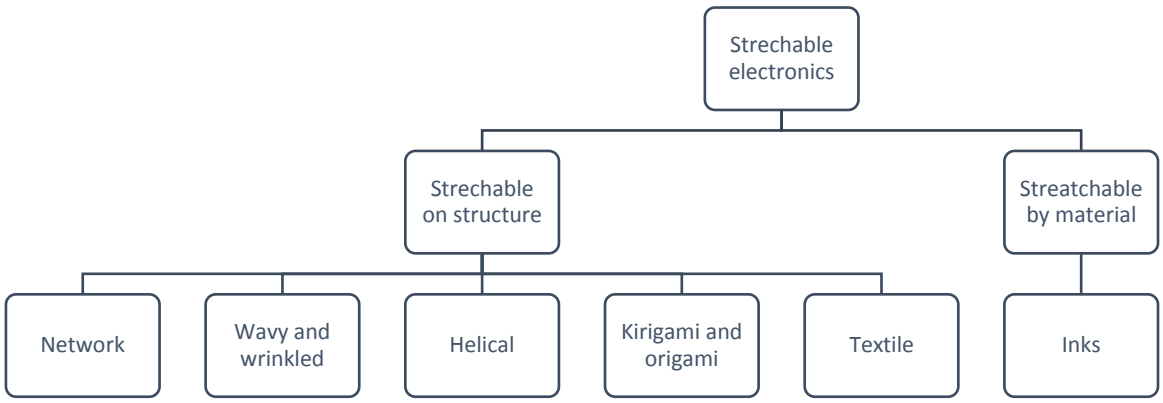

Fig 1. Stretchable electronics breakdown by conductive structure.

Figure 2 shows various stretchable electronics by structure. In section (a), we see biological tissue, e.g. skin structure, and its stress-strain curve. The curve is J-shaped and is imitated as closely as possible in biomedical, skin-related and e-skin applications. When stress-strain properties of electronics on the skin are similar to stress-strain properties of the skin, electronics are more comfortable to use. In (b) a network design structure is shown. It has a conductive pattern, network and structure on top of the elastic substrate. It can be stretched in different directions because of this structure. Section (c) displays a wavy and wrinkled design where the conductive material is wavy or wrinkled and lies on top of the elastic substrate. A wavy or wrinkled shape produces stretch, but it is strained only in a wave pattern direction. Section (d) shows a helical design structure where the conductors are in the air, on substrate or inside the substrate [5]. At (e) we see a kirigami and origami design, where the conductor and structure are so shaped that the structure picks up, bends or stretches. This design is reminiscent of paper folding. Section (f) shows different ways to pull the wire inside

the textile. Wires can be woven into textiles so that electronic circuits are built into the material. In this way the electronic circuit is part of a stretchable textile. [6]

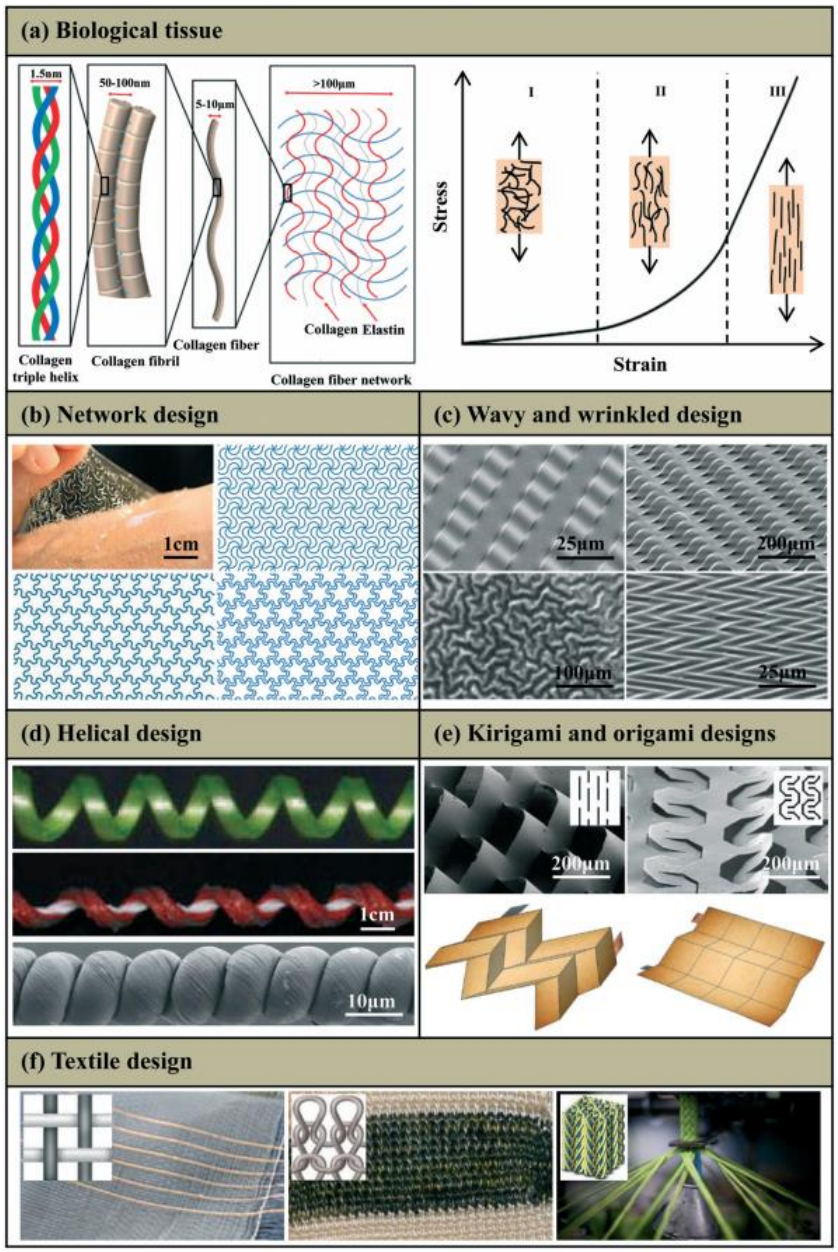

Fig 2. Structures of stretchable electronics [6].

The stretchable electrical line can also be realized with stretchable materials such as strain-conductive ink or fluid [7, 8]. When using this method, the ink or the fluid is printed onto the stretchable substrate. The structure of the conductive material should be such that it stays conductive in stretching and restores after the stretch. In addition, conductive ink or fluid should be compatible with the substrate and conductive material cannot be delaminated from the substrate by the stretching effect. Figure 3 shows a typical single-layer flexible electronics system, which has many similarities with stretchable electronics system structures [9]. Interconnections are only used in strain materials and structures.

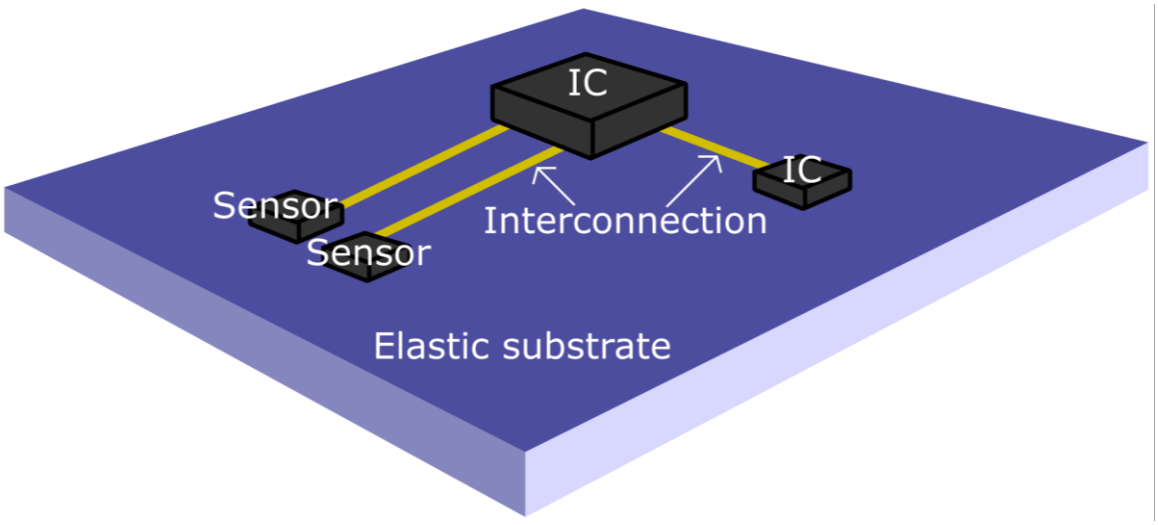

Fig 3. Typical printed flexible or stretchable electronic system.

This thesis focuses mainly on printed stretchable electronics which are based on structures on materials such as elastic substrates and inks, i.e. stretchable by materials and inks in Figure 1. IC circuits and their connection, as well as stretchable electronics based on structures, are excluded from this thesis.

2.1.1 History

Stretching electronics is a bit of a new research topic. The research on the subject can be considered to have its beginnings in the 21st century [10]. However, the first stretchable electronics application was seen in the 1930's when elastic telephone cords were made for telephones [11]. Stretchability of the telephone cords made it possible for the cord to automatically shorten itself when not in use and extended when the phone was used. The cord uses a helical design for stretchability. In addition, wearable electronics applications have been seen since in the 1960's. Such devices include wearable computers and activity trackers, for example. Also, e-skin has been developed since the 1970's [12].

Stretchable electronics has benefited from research on flexible electronics. Both of these are very similar: both have a flexible structure and use very similar materials, especially when these are manufactured by printing. The first flexible electronics research results were seen in the early 1990's when the flexible thin-film transistor was able to print on organic polymer and without any deterioration in performance in 1990 [10, 13]. Also, the first fully flexible light emitting diode (LED) was successfully manufactured in 1992 [10, 14]

The first modern stretchable electronics research began in the early 2000's when stretchable electronics were referred to as elastomeric electronics and studies focused only on elastomers rather than origami and kirigami design. This modern research aimed at the stretchability of internal components such as circuit boards. In the early stages of this research, a thin film conducting layer was attached on an elastomeric substrate such as PDMS (polydimethylsiloxane). This solution allowed a reasonably good stretch. Up to 25% to 40% of strain before the resistance increased considerably. In addition, the solution also carried good cycle testing. [15-17] Structurally stretchable electronics systems were hard components on soft and elastic substrates, like seen in Figure 3 [18]. The term 'stretchable electronics' became established in research in 2006–2008, when instead of elastomeric electronics, it was

called stretchable electronics in publications. However, both names are still used although stretchable electronics is more popular. Elastomeric electronics are only used in cases where stretchable electronics solutions with an elastic substrate are described, only in rare cases.

In recent years, several different applications have been seen in the field of stretchable electronics research. Stretchable batteries have been developed with origami structure, as well as using helical design between the battery shells [19, 20]. In addition, direct applications to the skin which are hidden in a tattoo as well as fully completely transparent e-skin applications have been seen [12, 21, 22]. Also, interconnections are achieved in different ways, in structures and stretchable inks and fluids, as previously stated. There have also been commercial products that utilize stretchable electronics. From these examples, the shorts which measure electrical activity produced by the muscles [23] are shown in Figure 4. Research into stretchable electronics has been conducted extensively in many different areas. This is a good basis for future research and development.

Fig 4. Shorts which measure electrical activity of muscles [23].

2.1.2 Future and possibilities

As stated at the end of the previous chapter, stretchable electronics have been researched in various ways. There is a variety of ready-made application for wiring, different substrates and stretching components. In addition, there are already individual products on the market that use applications of stretchable electronics. This creates a great potential for different applications, for example, in wearable electronics and medical applications, for which several different sensors have already been developed [24]. However, there is a need to research collecting and storage of energy, the performance and energy efficiency of components, as well as integration of different applications. However, all these should be done with utmost reliability and assurance that devices are able to withstand their intended use, like those designed to help monitor human health, for example. There is still a lot of clinical testing and validation ahead, because without it, the best potential applications may not be viable [24].

Stretchable electronics research is going to improve the well-being of all people and make these electronic devices more user-friendly. For their best applications, they will be integrated into clothes or even into the human body. Someday we will be able to use stretchable devices and track invisible sensors tracking our own health in real time. If necessary, electrocardiograms can be sent to doctors in real time and get a diagnosis without going to the doctor's office. In addition, we can monitor our body functions and controlled by drugs, before seizure even begins.

2.2 Fabrication techniques

This chapter examines the fabrication techniques used to manufacture stretchable electronics and generally various substeps of printing. Fabrication techniques with screen printing in conventional printing methods and inkjet printing in digital printing methods are covered. The chapter also deals with printing methods in general and how printing is done using different printing techniques.

2.2.1 Screen printing

Screen printing is one of the oldest printing methods. It has been used to create repeatable figures on textiles in Asian, African and European cultures since over 2000 years ago. In addition, it is one of the most versatile processes for transferring ink and it is still the most-used way to produce printed electronic circuits. It is suitable for productions ranging from extremely small components to those a few meters in width as well as long formats of production. Also, screen printing is a very easy printing method. If the ink and mesh are chosen correctly, non-trained people can print at an acceptable level of quality. [25, 26, 27]

Although the printing techniques differ from each other, generally each method has the same substeps of printing. Substeps of each printing can be divided into pretreatment and six different steps during printing. Substeps of printing are detailed in Figure 5 and shown in Figure 6. [25]

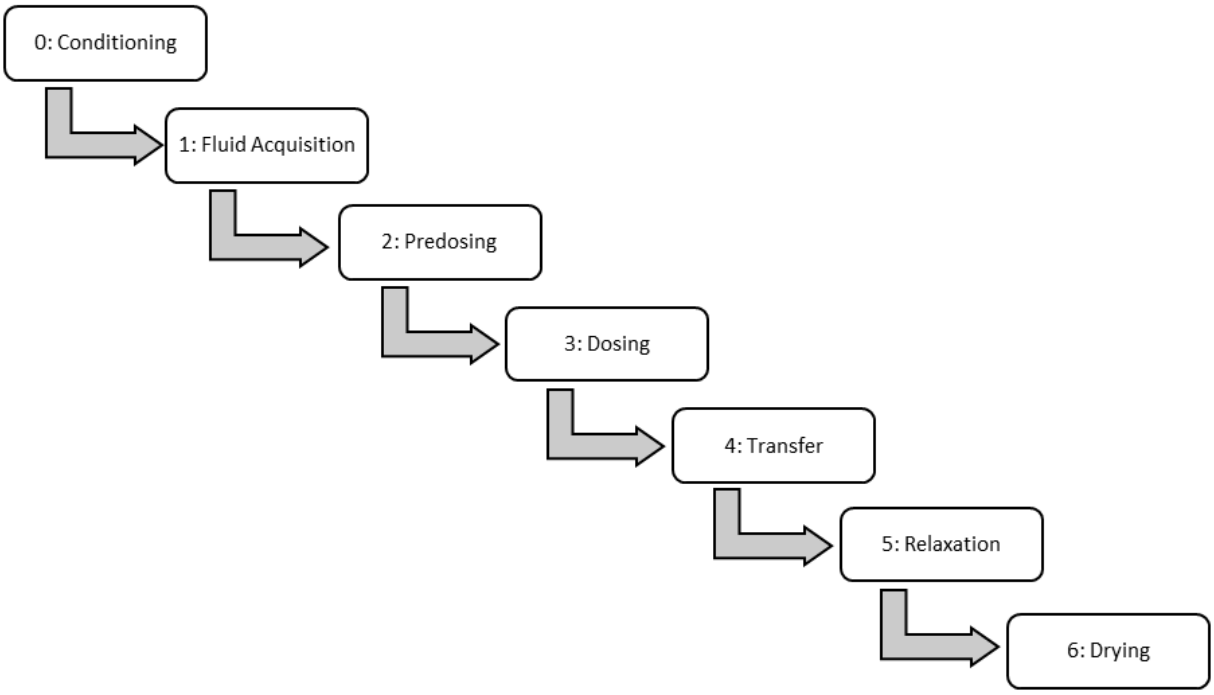

Fig. 5. Substeps of printing.

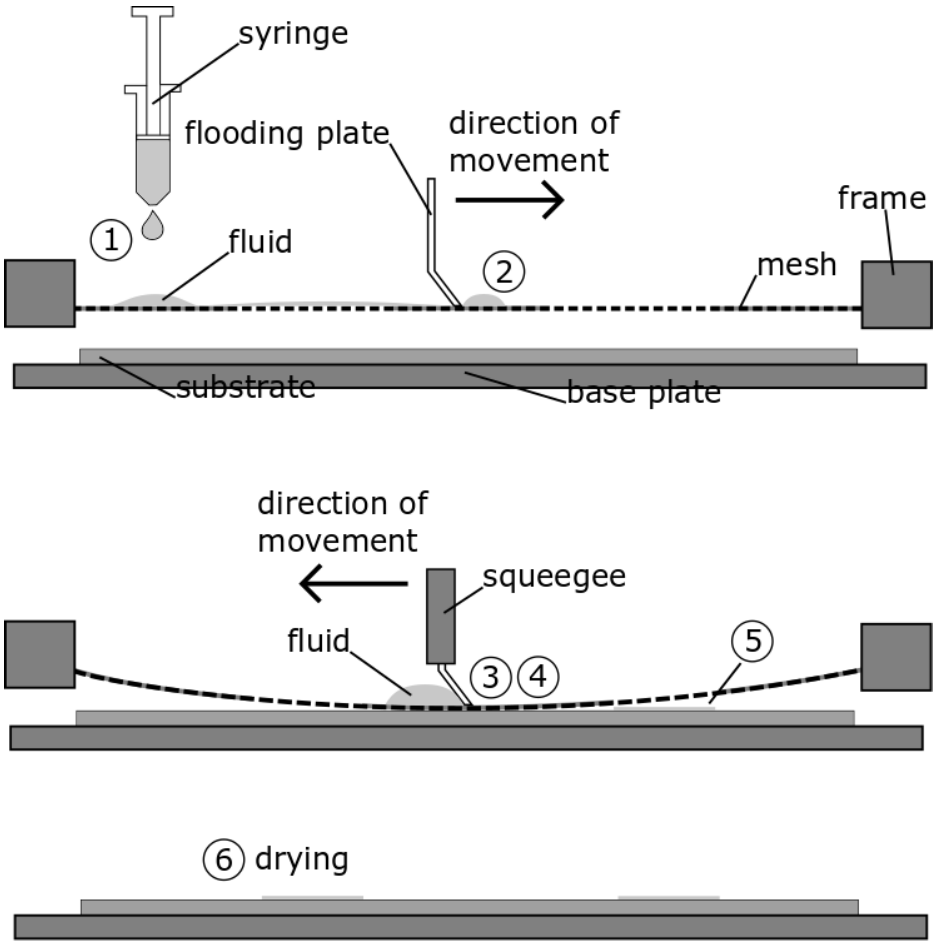

Fig 6. Substeps of the screen printing process [25].

The principle of screen printing is very simple and is shown in Figure 6. It consists of a screen, a squeegee, a flooding blade, a substrate holder and pretreatment and six different substeps. At first substep 0: Conditioning (of the Printing Fluid and Substrate Pretreatment) happens before actual printing. The packaged substrate sheets or roll have to be individually separated or unrolled. Their surface impurities must be removed, which have resulted from production process or from storage and the substrate is prepared for printing. Ink has to be selected and prepared for printing. Wetting properties of the substrate have to be right for the used ink. More wetting properties can be seen in chapter 2.3. [25, 26, 27]

The substep 1: Fluid Acquisition is a step during which fluid is prepared for ink transfer. In this step, a specific amount of fluid or ink is supplied on the mesh or the screen in screen printing (number 1 in Figure 6). The screen is shown in Figure 7. In (a) it is seen from the print side and in (b) it is shown as a cross-sectional view of the screen. [25, 26, 27]

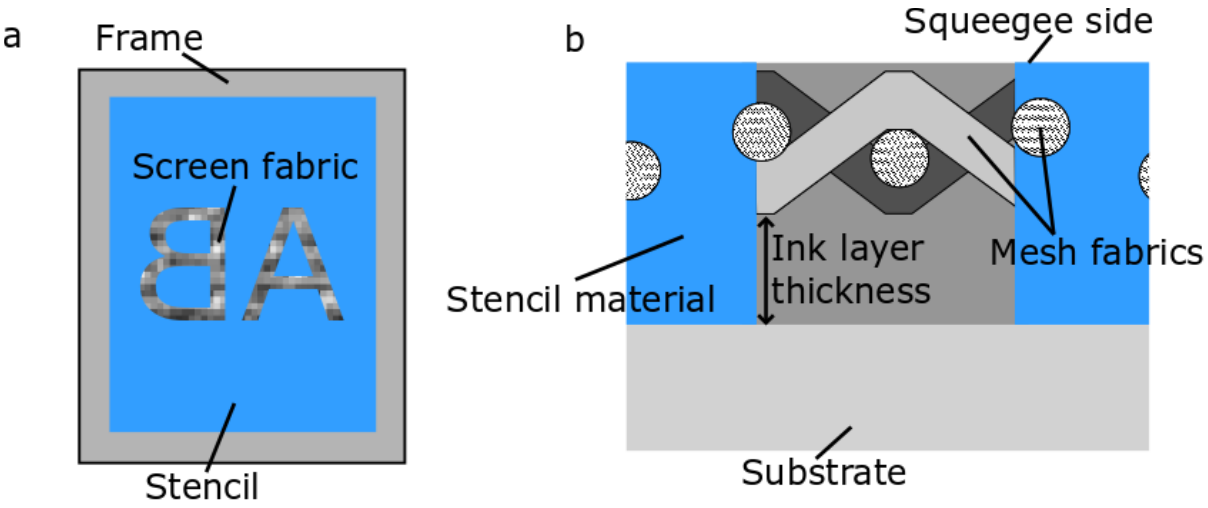

Fig. 7. A screen for screen printing [27].

In substep 2: Predosing fluid is divided and distributed such that it can be applied to the printing form when the whole mesh is flooded with ink using a flooding blade (number 2 in Figure 6). This step guarantees that the printing form acquired the desired amount of the printing fluid. [25, 27]

In substep 3: Dosing (of printing fluid) is a step during which each point of the printing form's surface acquires a specific quantity of printing fluid. The squeegee presses the ink through the mesh at the printing areas (number 3 in Figure 6). Mesh in the screen is not against the substrate, but stencil material creates a little gap between the mesh and substrate like in Figure 7b. [25, 27]

In substep 4: Transfer, the desired quantity of printing fluid is transferred to the intended point onto the substrate. This step happens at the same time as the squeegee presses the fluid onto the stencil and contacts the substrate. When a contact between substrate and fluid is created, air and other particle contaminations are supplanted from the substrate. For a short moment, the wetting properties of the substrate are fully independent of any equilibrium properties. This means that wetting of a substrate is enforced. When the force used to transfer the fluid is removed, the enforced was dissolved. At the end, the mesh is lifted and the ink adheres to the substrate (number 4 in Figure 6). [25, 26]

The liquid on the substrate surface is free, highly mobile and susceptible to impurities from the air. Impurities change the surface energy of the liquid–gas interface in the liquid film. Stability of the liquid film can change to become unstable if wettability is insufficient. In addition, the phenomenon of viscous fingering is common in conventional printing methods, which means that the fluid film is unideal. In substep 5: Relaxation minimizes the phenomenon of viscous fingering. In this step of the process, a short period of time passes before the fluid relaxes, which means that the fluid surface has levelled out (number 5 in Figure 6). Relaxation time depends on the viscosity of the fluid and the area of the fluid. More information on fluid relaxation is found in chapter 2.3. If the conditions for wetting are insufficient in the substrate, the substrate and the conductive fluid can occur. This causes interconnections to have nonconductive parts. [25, 26]

The last substep 6: Drying, as stated in its name pertains to drying the fluid. In this step, solvent residuals from the printed film are evaporated and the fluid hardens. This means that the fluid or the film is already solidified, which further means that capillary transport of printing fluid is impossible. In drying, one possible way is to utilize an additional heat source in order to accelerate the process. This is also called the thermal post treatment. Thermal post treatment not only eliminates solvent residuals, it also cures the printed film. [25, 26]

Challenges of screen printing are in mesh and ink selection. The mesh size and the ink should be selected according to each items' features. If particle size of the ink is large, the mesh size should also be large. The general rule is that width of the mesh should be at least three times larger than width of the ink particles. Smaller mesh is easily blocked by ink particles. However, the mesh must not be too large because elsewhere the ink will pass mesh without squeezing and pressure. In addition, the mesh should be sufficiently stiff, but not have too wide threads. Too slack mesh and too much pressure by the squeegee can cause inaccuracy at the edges of the printed areas, known as blur. Metal is generally used as the mesh material nowadays, because of its chemical stability and its durability. In Figure 7 the mesh geometry is shown, for which w is mesh width, d is thread thickness and a is thread spacing. The ink should be selected with an appropriate particle size, as previously mentioned. In addition, ink viscosity should be appropriate. About 500 to 5000 mPa-s of viscosity inks are usually used in screen printing, but up to 50000 mPa-s inks can be used. [25, 26, 27, 28]

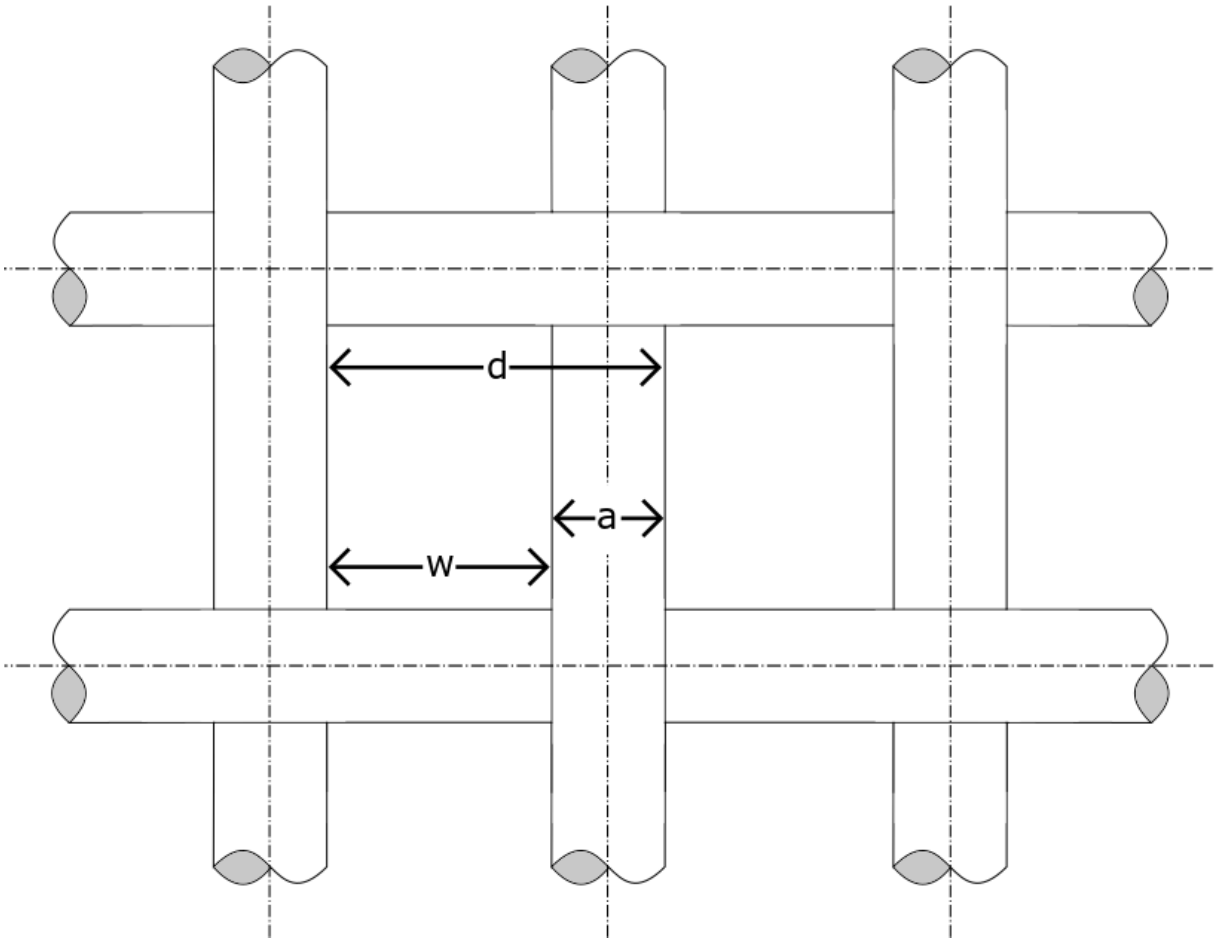

Fig. 8. The mesh geometry [27].

Screen printing is a slow method for high-volume manufacturing, so it can be upscaled by the roll-to-roll printing method. Roll-to-roll or rotary screen printing methods have a rotating screen that works like a printing mesh. A printing fluid is fed inside the cylinder which is pressed by a squeegee into the desired shape onto a substrate as shown in Figure 9. After printing, the printed fluid is allowed to relax and dry by a heating furnace. The roll-to-roll method can be used to print large quantities quickly and cost-effectively compared to sheet screen printing. [29]

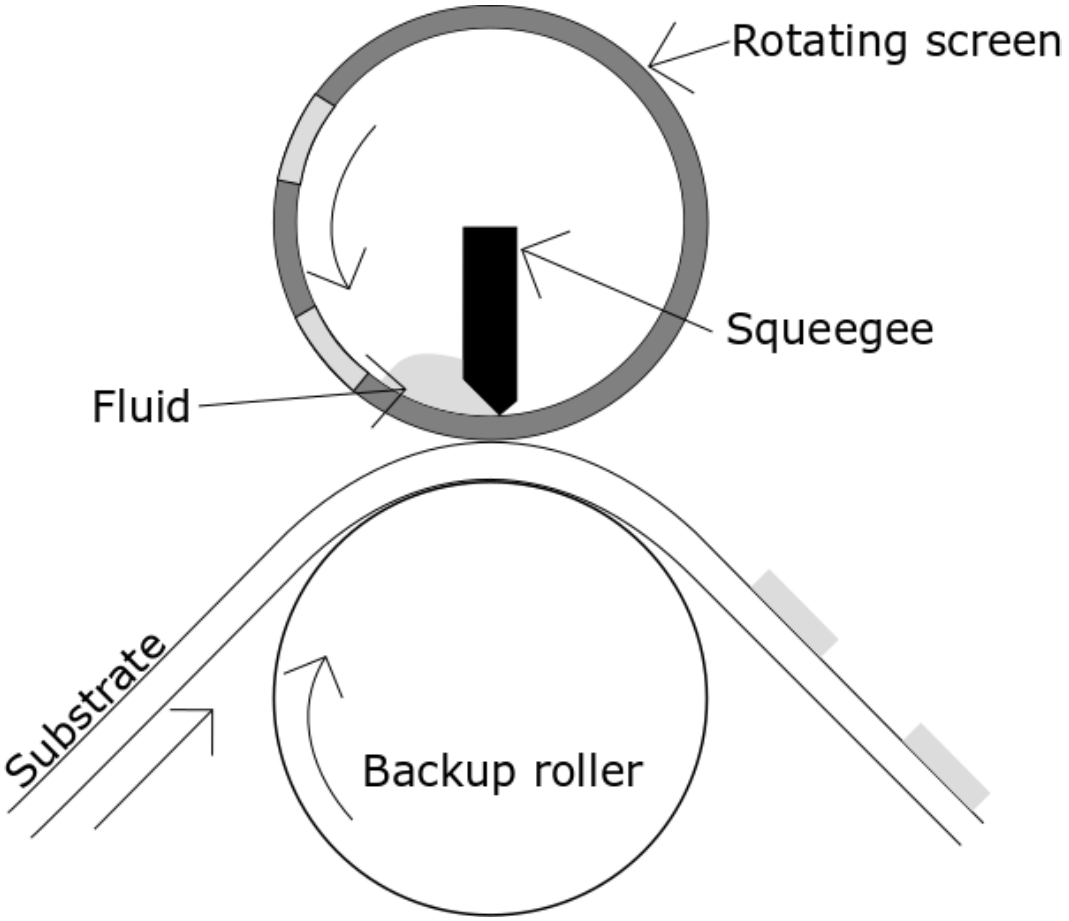

Fig. 9. Principle of rotary screen printing.

2.2.2 Inkjet printing

Inkjet printing is the most commonly used technology for digital printing systems. The first patent for inkjet printing was in 1951, so it is a quite new printing method. In inkjet printing, ink is sprayed from nozzles, which means that no image carrier is needed. Inkjet printing technologies can be divided into two main categories, continuous inkjet and drop on demand inkjet, like in Figure 10. [25]

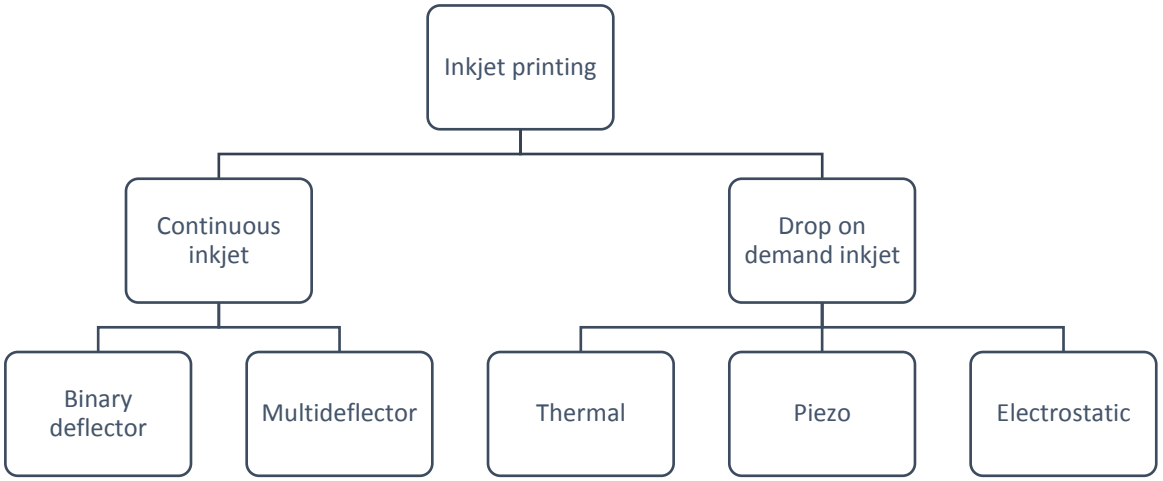

Fig. 10. Categories of inkjet printing.

Continuous inkjet, as stated in its name, feeds continuous ink from a nozzle. The desired ink droplets are released onto the substrate and unneeded ink droplets are removed before contacting the substrate by the charge electrode, deflector and gutter. The principle of continuous inkjet technology is shown in Figure 11. [25, 27]

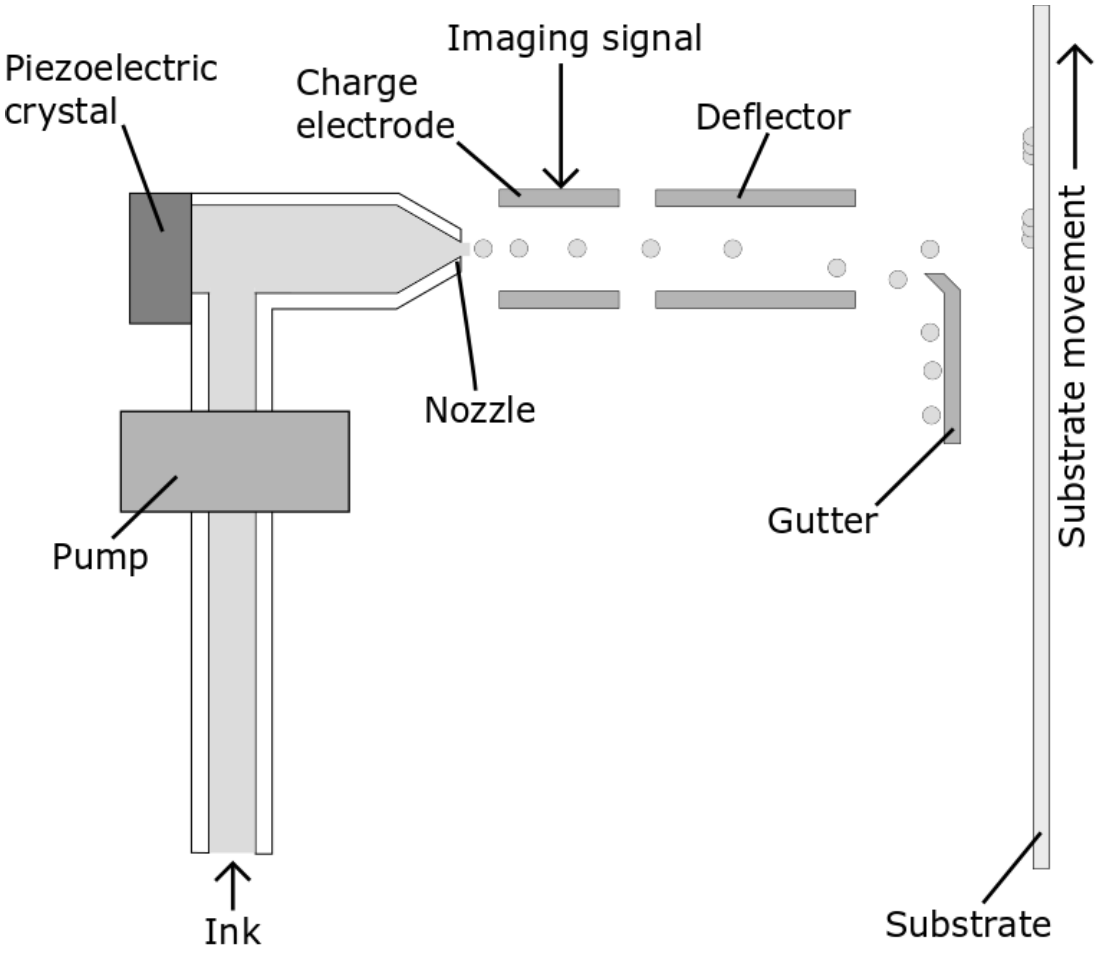

Fig. 11. Principle of a continuous inkjet [27].

Drop on demand, also known as DOD inkjet, differs from continuous inkjet. In the DOD method, a print head releases ink droplets only when needed on the substrate. The print head is the printing unit which contains an ink supply channel, an electromechanical actuator circuit and the nozzles. The principle of a DOD inkjet with a piezo is shown in Figure 12. [25]

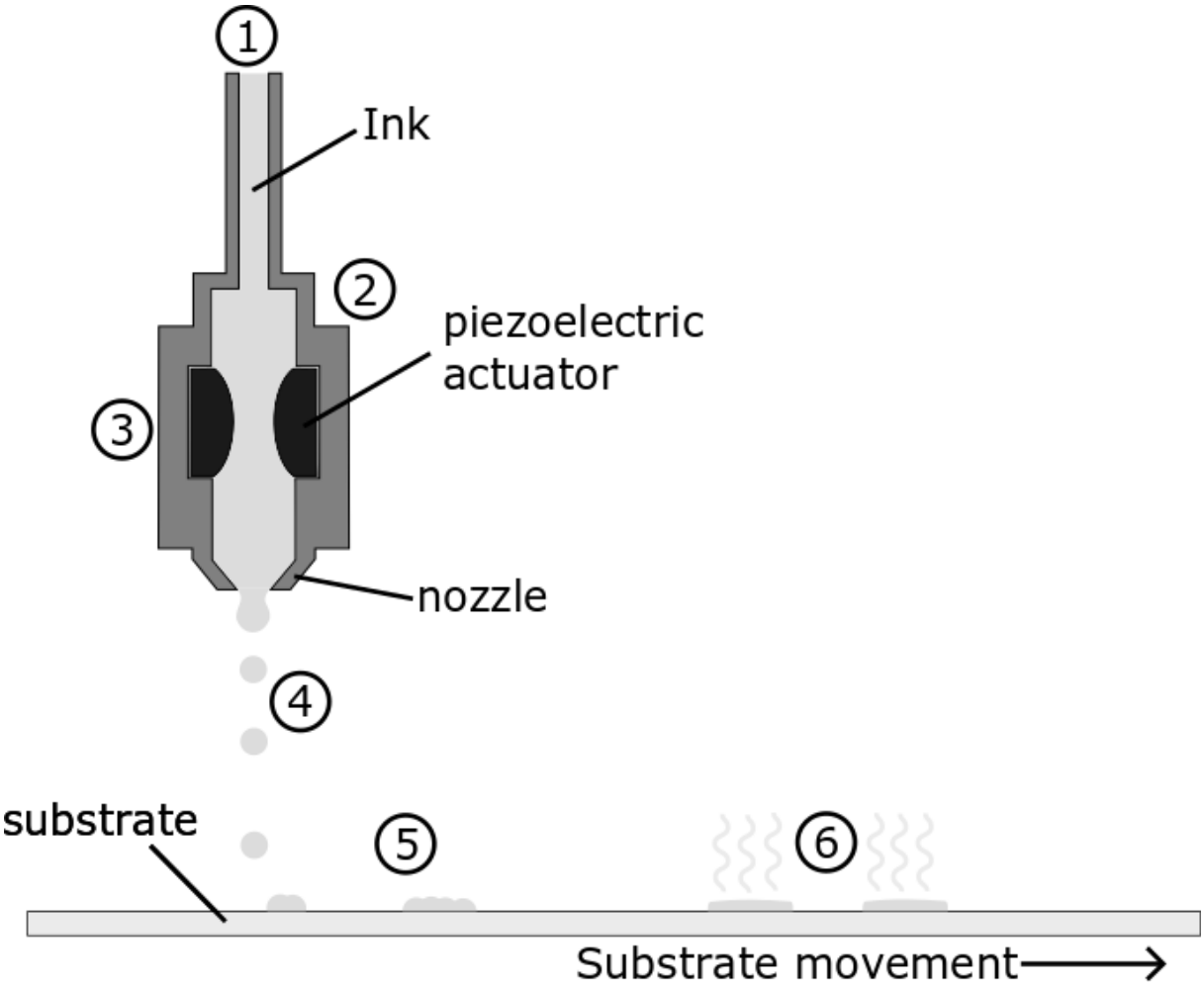

Fig. 12. Principle of a drop on demand inkjet [25].

The substeps in inkjet printing are very similar to the silk screen printing process, but not so clearly. In inkjet printing, the first step is to fill the ink cartridges connected to the print head with homogenized ink of the correct viscosity (number 1 in Figure 12). In the following step, the ink is transferred onto the substrate in several steps at the same time and steps are not clearly separable. At number 2 in Figure 12, ink is in the ink channel and at number 3, internal pressure is changed which forwards the ink to the nozzle. Internal pressure could be created with the piezo or thermal element, for example. Pressure causes the ink droplet to move from the nozzle to the substrate (number 4 in Figure 12). Then inks are relaxed (number 5 in Figure 12) and dried (number 6 in Figure 12) on the substrate. [25]

Challenges of inkjet printing are ink preparation and selection. The ink has to be prepared and selected so that it can pass through the nozzle and not block it. Also, the ink must not be of a runny consistency so that the nozzle does not drop unwanted ink droplets. For high

viscosity inks, a larger nozzle should be chosen. Different inkjet processes are typically used for inks with a viscosity value of about 1–30 mPa-s [27].

2.3 Material properties

This chapter examines the properties of materials and how the properties of materials affect the manufacturing process, the application and reliability. Each printing process requires certain properties of the materials, and in particular the substrate surface and printing fluid. Of course, the requirements and desired properties of the application also affect the choice of printing fluid and substrates.

Ready-to-print inks are rarely offered by manufacturers. In general, ready-to-print ink qualities vary, which is the reason why manufacturers do not favor delivery of ready-to-print inks. In general, the inks are delivered as solid materials that the end user must handle as fluid to make ready for printing. Especially in research applications, the printing fluid composition is controlled. In order for the printing fluid to be printed reliably on the substrate and for it to harden on the substrate surface as desired, as well as and reliably adhere to the surface of the substrate, the printing fluid and the substrate must have suitable properties. Printing fluid properties have an impact on printing, relaxation and drying as well as conductivity of printed film. Especially, viscosity and surface tension have an essential effect on ink transfer to the substrate. Solvents can change viscosity and surface tension of printing fluid. The electrical conductivity is influenced, among other things, by the size, density and distribution of particles in a given surface area. The ratio of solvents and binder can be affected by levelling of the surface and drying, improving film formation, particle scattering and wetting properties. All of the above things have an effect on the behavior of the material during stretching in addition to relaxation and drying. [8, 25, 26, 30]

Viscosity determines a fluid's ability to transfer mechanical stress and hydrodynamic pressure to the substrate through the liquid phase at a given velocity [25]. In other words, with higher viscosity, the ink is stiffer. Viscosity can be mathematically determined by imaging a cube with isotropic fluid inside. The cube is plotted in a normal Cartesian coordinate system. The faces of the cube have a given size A_i, where $i = x, y, z$. By pressing the two opposing sides of the cube by force ΔF_j, a shear flow is generated inside the fluid. This shear flow is the gradient of the flow velocity for which a shear rate γ can be determined, like in equation (1). [25, 26]

$$\gamma_{ij} = \frac{\partial v_i}{\partial x_j} + \frac{\partial v_j}{\partial x_i} \tag{1}$$

Dynamic viscosity η can be solved in shear stress τ equation (2),

$$\tau_{ij} = \frac{\Delta F_j}{\Delta A_i} = \eta \gamma_{ij} \tag{2}$$

where F_j is tangential force and A_i is face size [25]. Dynamic viscosity is usually given in units of Pa-s. Shear force and shear stress are tensor valued quantities which mean that $\tau_{ij} = \tau_{ji}$ as well as $\gamma_{ij} = \gamma_{ji}$. [25]

Equations (1) and (2) work very good and have high accuracy with Newtonian fluids, which have a constant dynamic viscosity at a given temperature. Many printing fluids are

non-Newtonian which means that their dynamic viscosity depends on shear rate. Dynamic viscosity of non-Newtonian fluids can be solved in equation (3). [25, 26]

$$\eta = \eta_{ref} \left(\frac{\gamma}{\gamma_{ref}} \right)^{\alpha} \tag{3}$$

In equation (3) η_{ref} is the measured nominal viscosity of the defined reference shear rate γ_{ref}. Dynamic viscosity η is given from equation (2). Exponent α is a value which describes shear thickness. It is 0 for Newtonian fluids, $\alpha > 0$ for non-Newtonian fluids whose viscosities increase with increasing shear rates and $-1 < \alpha < 0$ for non-Newtonian fluids whose viscosities decreases with increasing shear rates. [25]

Some fluid types are used in printed electronics, the viscosities of which cannot not be fully characterized by a scalar viscosity. These fluids are referred to as anisotropic, complex or mesogenic liquids. [25]

The surface tension or surface energy refers to any liquid interface that exerts a mechanical stress to the environment, for example, different materials or different phases. The surface tension minimizes the size of interface and this refers to liquid-liquid, liquid-gas and liquid-solid interfaces. On a curved surface, the surface tension can occur at a force per surface area that is normal on the surface. Direction of the force depends on the surface. If the surface is convex, the force is directed toward the liquid and if the surface is concave, the force is directed into the surrounding gas. Because of this, the drop of water tends to attain a spherical shape and minimizes its surface at a given drop volume. In this case, the surface tension inside the drop of water or liquid may be calculated from the equation for Laplace pressure,

$$p_L = \frac{2\sigma}{r} \tag{4}$$

where p_L is Laplace pressure, σ is surface tension and r is radius of the liquid drop. [25, 26]

Depending on the used printing method, printing fluid selection should take into account the requirements of the printing method. The range of surface tension and viscosity are different in different printing methods. Too high viscosity and too high surface tension can cause the printing fluid to block the printing machine nozzle or the printing fluid will not adhere to the substrate surface, for example. Too low surface tension and too low viscosity can also cause the printing fluid to spread and the resolution is weakened, or in the worst case, the printing head or screen drops unwanted ink droplets and spoils the whole print sample. The generally used range of surface tension and range of viscosity for different printing methods are in Table 1. [25, 26]

Table 1. Parameters of different printing methods [25, 26, 31].

Printing method	Surface tension (mN/m)	Viscosity (mPa-s)
Screen	23-35	500-50000
Inkjet	18-40	1-30
Gravure	18-40	1-200
Flexo	18-40	1-500
Offset	23-45	2000-100000

Wetting of the printing fluids and the substrate surface is one of the principal properties for the quality of printing. Wetting is defined as the ability of a liquid to supplant a competing from a solid surface and to bring the interfaces between the three participating phases [25]. It

can be characterized by surface tensions of the respective interfaces like in the Young's equation,

$$\sigma_{LG} \cos\theta = \sigma_{SG} - \sigma_{SL} \tag{5}$$

where θ is the contact angle between the substrate plane and the tangent at the liquid-gas interface. In equation (5), σ_{LG} is the surface tension in liquid-gas interface. σ_{SG} and σ_{SL} are surface tensions in substrate surface-gas and substrate surface-liquid interfaces. [25, 26]

Wetting properties are also possible to characterize by the wetting parameter *S*, like in equation (6). If $S > 0$, that is the preferred perfect wetting. [25]

$$S = \sigma_{SG} - \sigma_{SL} - \sigma_{LG} \tag{6}$$

Energy $W_{LS}^{(adh)}$,which requires that the printing fluid is adhered onto the substrate surface, can be calculated in equation (7). [25, 26]

$$W_{LS}^{(adh)} = \sigma_{SG} + \sigma_{LG} - \sigma_{SL} = \sigma_{LG}(1 + \cos\theta) \tag{7}$$

From equations (7) and (8) it is seen,

$$\sigma_{LG} \gg -S > 0 \tag{8}$$

that a large surface tension σ_{LG} in the liquid-gas interface without perfect wetting corresponds to a small contact angle and a reasonably large energy of adhesion which are optimal to printing. [25]

The printed layer surface remains waved, like in Figure 13. This waved surface may be caused from viscous fingering or hydrodynamic instability [25, 26]. With relaxation time, we can influence the leveling of the surface. For example, a sinusoidal height function $h_1(x,t)$ can be considered with wavelength λ and amplitude $A_\lambda(t)$ of the x modulation. The height function is shown in equation (9). [25]

$$h_1(x,t) = A_\lambda \sin 2\pi x/\lambda \tag{9}$$

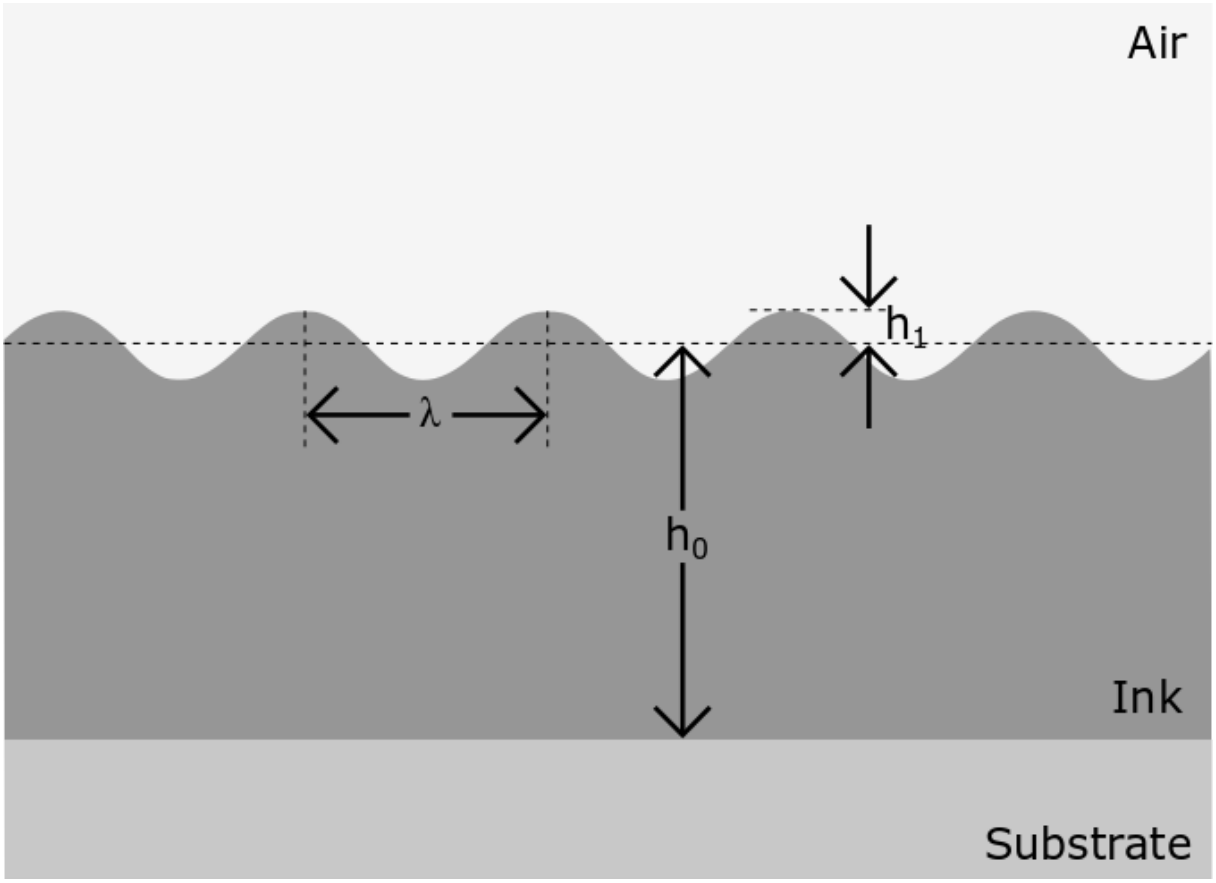

Fig. 13. Wavy printed layer [25].

Relaxation timescale is shown in equation (10).

$$\tau_{\lambda}^{rel} = \frac{3\eta\lambda^4}{16\pi^4\sigma h_0^3} \tag{10}$$

Like in equation (10), this waved surface will smooth out exponentially in time. The relaxation time τ_{λ}^{rel} increases by fourth order in λ, because capillary forces are more effective in small wavelength and slower for larger wavelengths. The typical relaxation time is milliseconds if the wavelength is in the micrometer range, but in the millimeter several minutes are needed. Also, the relaxation is not so effective on very thin liquid films as on thicker ones. [25]

In some printing methods, such as inkjet printing, the effectiveness of relaxation should be taken into account. Inkjet printing deposits some arrays of liquid drops, which means that the time between two drops cannot be too long, because elsewhere the film thickness has appreciably changed. If it has appreciably changed, viscous fingering may occur. Viscous fingering wavelength λ_{vf} is shown in equation (11),

$$\lambda_{vf} \sim h_0 \left(\frac{\eta v_p}{\sigma}\right)^{-0.5} \tag{11}$$

where v_p is printing speed. According to equation (10), viscous fingering within the timescale τ_{vf}^{rel} is shown in equation (12),

$$\tau_{vf}^{rel} \sim \frac{h_0 \sigma}{\eta} v_p^{-2} \tag{12}$$

in which we see that the viscous fingering problem can be reduced by increasing printing speed. [25]

Marangoni effect can also cause a waved surface and this happens in the drying process. It means that some solvent is evaporated, the volume of the foil decreases, concentrate increases and this affects surface tension. The Marangoni effect can be characterized like in equation (13).

$$\tau_{\lambda}^{m} = \frac{\lambda^2}{2\pi^2 h_0 \sigma_{\emptyset}} \tag{13}$$

Conductive particles of ink affect conductivity and stretching. The particles are many different shapes, for example sticks, balls and flakes as well as their combinations. Each of them works differently in stretching and affects the resistance of the conductive layer. Silver-based inks are very popular in stretchable research applications because silver-based inks have well-established understanding [30].

The polymers are in the prime position as a substrate material when talking about printed and stretchable electronics. Examples of such polymers are PET (polyethylene terephthalate), TPU (thermoplastic polyurethane) and PDMS. Polymers are the basis for many stretchable electronics applications as well as semiconductors and dielectrics. Wetting properties and stretchability are also essential properties of the stretchable applications. These properties can be changed in the polymers by, for example, using solvents. [25]

3 MEASURING STRETCHABLE ELECTRONICS

This chapter deals with the measuring of stretchable electronics. It deals with reliability and what it is, and why testing is done. Also, it deals with failure mechanism and causes of failures. In addition, we look through stretchable electronics testing standards, as well as how major organizations do testing and measurements.

3.1 Reliability and testing

In the simplest way, r*eliability is conformance to specification over time* [32, 33]. However, it can be assumed that with reliability there is as little as possible uncertainty about things. These things can mapped out by reliability testing and try to become aware of a product's ability to function. But why do we want to find out these uncertainties? The more awareness of a product's ability to function is, the better its operation time and failures can be predicted. This can be used to estimate whether the product is operating at a desired service life, as well as cost of the reliability and total costs. Figure 14 shows the impact of costs on reliability. The picture shows the increase in quality and reliability costs over the total cost. [34]

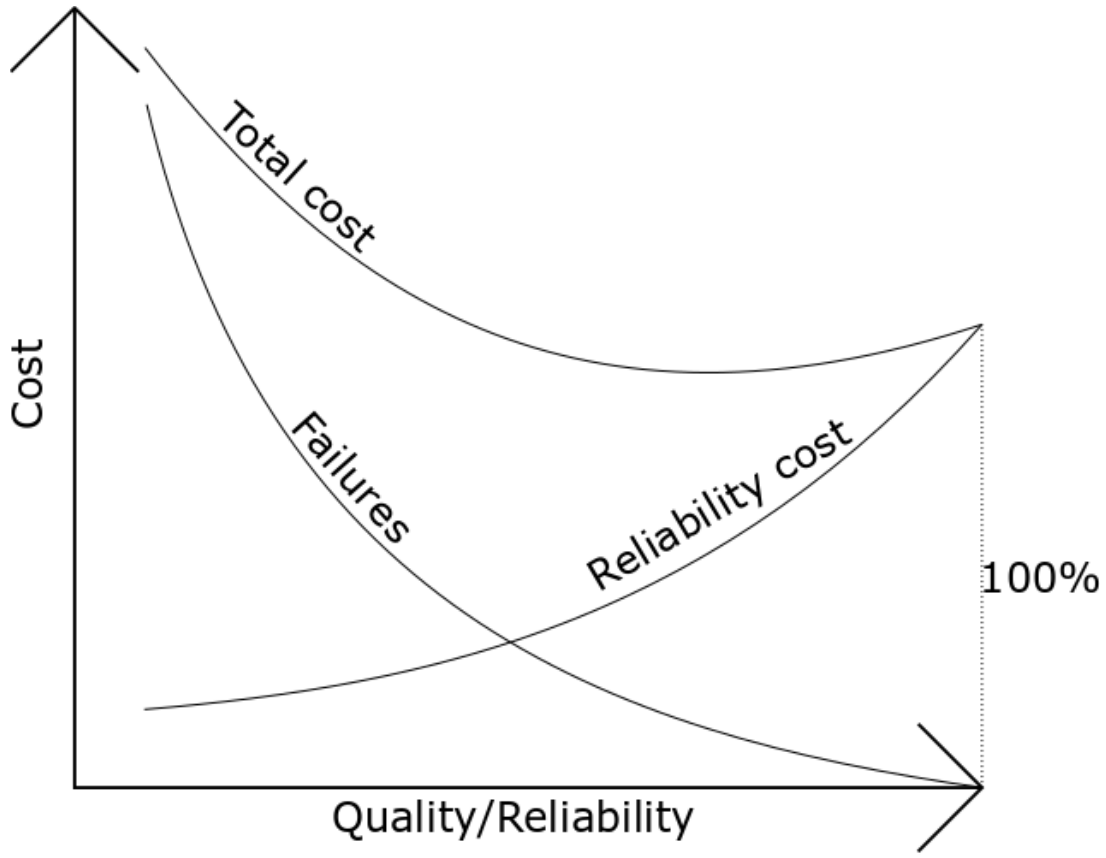

Fig. 14. The impact of reliability on costs [34].

Reliability should be assessed at each stage of the process. This includes any change in the product and manufacturing, changing the reliability of the product and increasing or altering the possibility of chance of failure. Figure 15 shows process flow of the printed electronic system. Reliability can be tested after each process and when the product is ready. Good material preparation and the right material choices play a major role in product reliability,

especially in flexible electronics. Also, the used printing method and the print quality affect the reliability of the product. These failures and failure mechanisms are discussed in more detail in chapter 3.2. Reliably performing each process, reliability testing, and coordinating all stages will ensure a reliable result. Assembly of components and finishing, such as lamination, are excluded from this thesis.

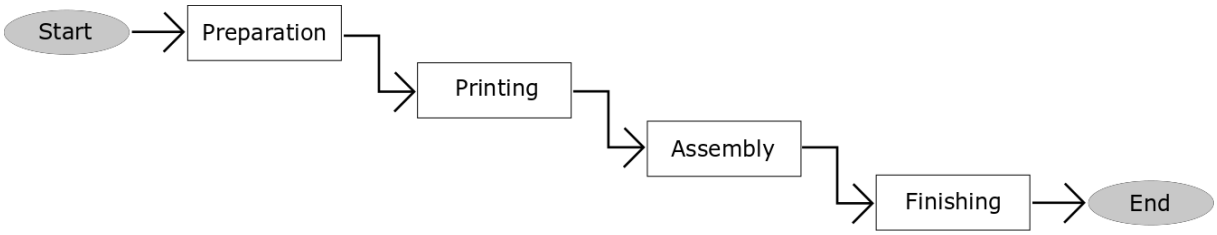

Fig. 15. Process flow of printed electronic system [25].

Product useful life can be estimated in time, for example in hours, days, or operating cycles, for example, and how many presses the button lasts or how many stretches a stretchable electronic device can withstand. Incidence of failures and reliability can be divided into three stages. Infant or early failures are failures that occur at the beginning of the product life cycle. Usually these failures occur due to failures in components or production. Random failures can occur at any stage of the product life cycle. These random failures are the main causes of device malfunction during its useful life. They cannot be anticipated and their cause is unknown or their cause is very difficult to determine. Attempts can be made to minimize these random failures by selecting high-quality materials and to distribute the load of the product correctly. Time-dependent failures occur at the end of the product life cycle. These failures are caused because components wear out over time and cycles. Failure rate is shown in Figure 16 where the failures are divided into three stages. If failure rate follows Weibull's distribution, failure rate at different stages can be analyzed by the equation (14),

$$\mathrm{r}(y) = \beta\alpha(\alpha y)^{\beta-1}, for\ y > 0 \tag{14}$$

where α is the scale parameter and β is the shape parameter. If the shape parameter β is lower than 1, failure rate decreases over the time. On the other hand, if the shape parameter is greater than 1, the failure rate increases. This is also shown in the bath-tub curve, in Figure 16. [32, 34-36]

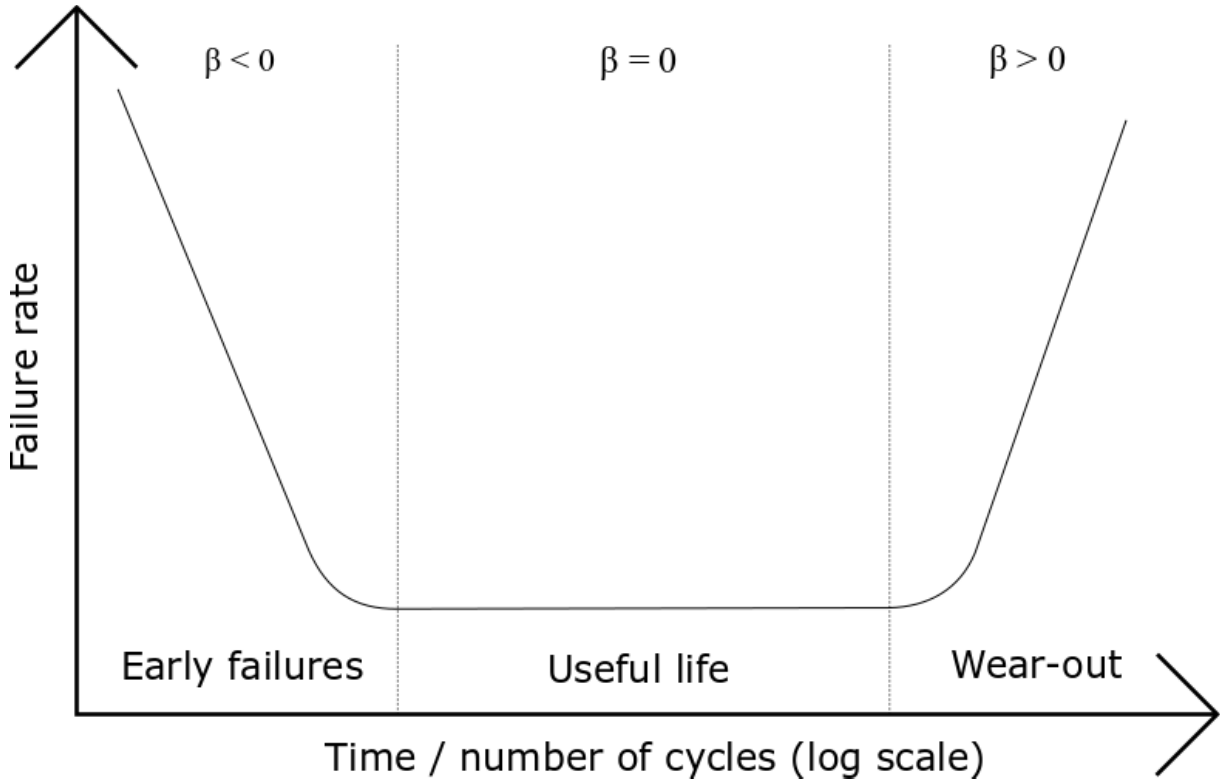

Fig. 16. The bath-tub curve [32].

The occurrence of failures and the reliability of the product during the life cycle can be analyzed by Weibull's distribution. The cumulative distribution function of Weibull's distribution is shown in equation (15). [32, 35]

$$F(y) = 1 - e^{-(\alpha y)^{\beta}}, for\ y \geq 0, where\ \alpha, \beta > 0 \quad (15)$$

The scale parameter α can be used to estimate the useful life of a product. α^{-1} is the value where 63.2% of the products have failed. The higher the α^{-1} value, the more durable the product is and the longer time or the more cycles the product can be expected to withstand. For example, if α = 1/1000, it can be assumed that about 63.2% of the products will fail after one thousand test cycles. Cumulative failure rate with a few different scale parameter is shown in Figure 17. [32, 35, 36]

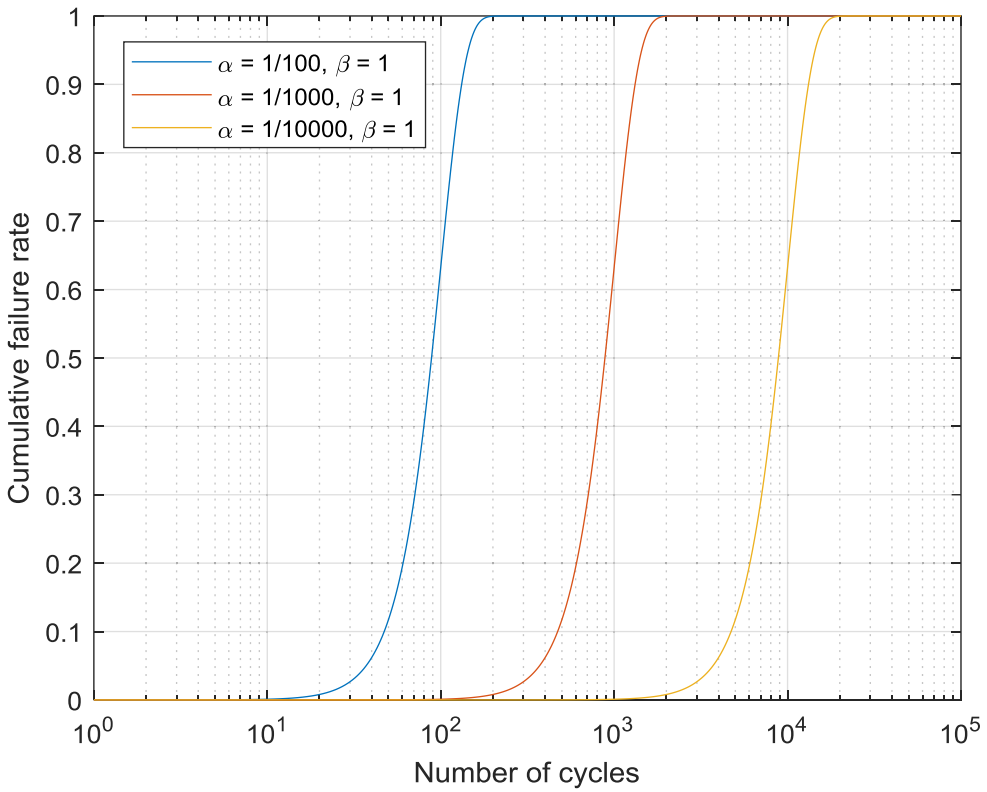

Fig. 17. Cumulative distribution function with varying scale parameter α.

The shape parameter β can be used to predict the distribution of product failures for different time periods or cycles. As can be seen from equation (15) and Figure 18, the greater the shape parameter is, the shorter the time or cycle intervals during which failures occurs and the easier it is to forecast the useful life of the product. [32, 35]

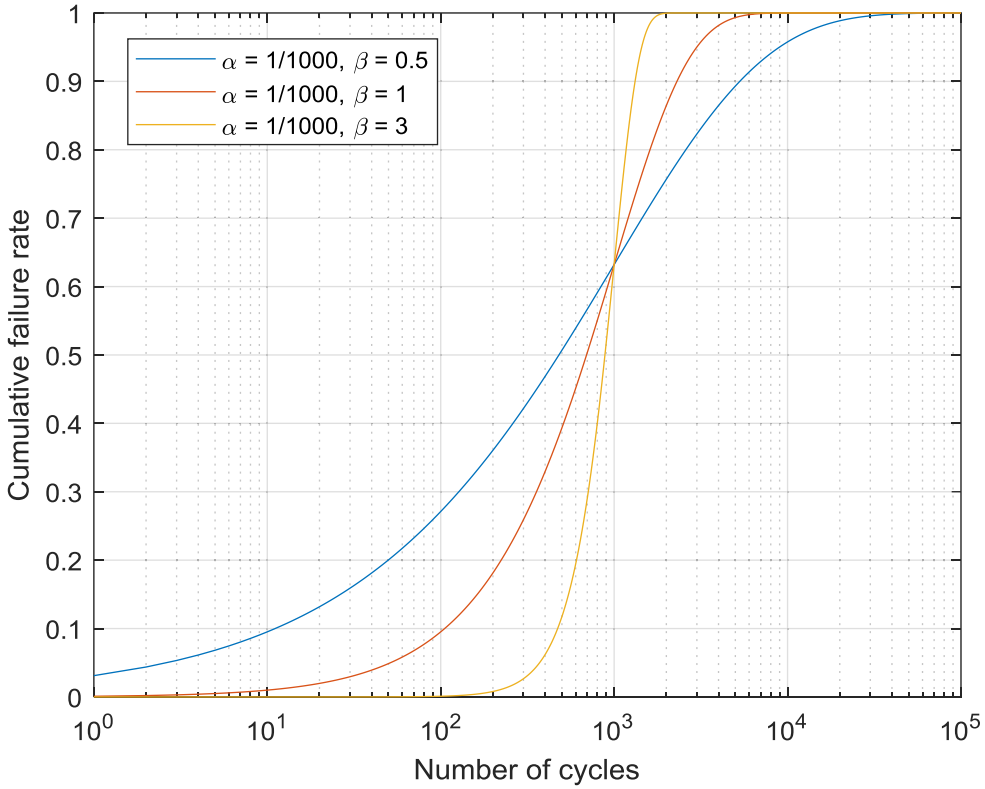

Fig. 18. Cumulative distribution function with varying shape parameter β.

How many similar samples should be tested to ensure the result can be considered reliable? This depends on the desired confidence level as well as reliability level and sample size. Confidence level describes the distribution of results. In general, the 95 % confidence level is used in research, which means that 95 % of the results would be within the confidence interval. The confidence interval can be calculated using equation (16) when there are more than 30 tested samples,

$$\overline{\mathrm{X}} \pm z\frac{s}{\sqrt{n}} \tag{16}$$

where $\bar{X}$ is the average of the measurement results and z is standard normal distribution value for confidence level; Table 2 contains commonly used confidence values. s is standard deviation and n is sample size. Minimum sample size n_0 can be calculated in equation (17),

$$\mathrm{n}_0 = \frac{\ln(1-c)}{\ln R_s} \tag{17}$$

when we know the desired confidence level c and the sample reliability R_s. Reliability level is the value of a product's reliability, that is, a value describing random and systematic errors. [37, 38]

Table 2. Commonly used confidence values and their normal distributions.

Confidence level	z value
90 %	1.645

95 %	1.960
99 %	2.576

3.2 Failure mechanisms

In general, failure mechanisms are ways, things or process resulting in failures. This can be, for example, electrical, physical, chemical, thermodynamical or other processes which cause failures. Failure mechanisms can be categorized into two groups: overstress and wear out mechanisms. If a failure is caused by a single load or stress, it is referred to as overstress failure. For example, a too long strain or a too hot washing machine program for stretchable electronics system is referred to as overstress failure. The wear out mechanism, according to its name, refers to when products or systems wear out. This may be, for example, due to fatigue or corrosion or too many stretches for a stretchable system. In reliability testing, we try to find these limits for products; how long a product can withstand strain or how many stretches a product can take before it fails. [39]

What types of failures occur in strain tests? For soft substrate-printed stretchable and bendable wire structures, failures can be categorized in four different modes based on the failure type. These failure modes are stretching are cracking, slipping, delamination in a slipping zone and delamination. Usually, more rupture or cracking occurs in thin conductive layers while with thicker layers delamination is more common, as shown in Figure 19. [32, 40]

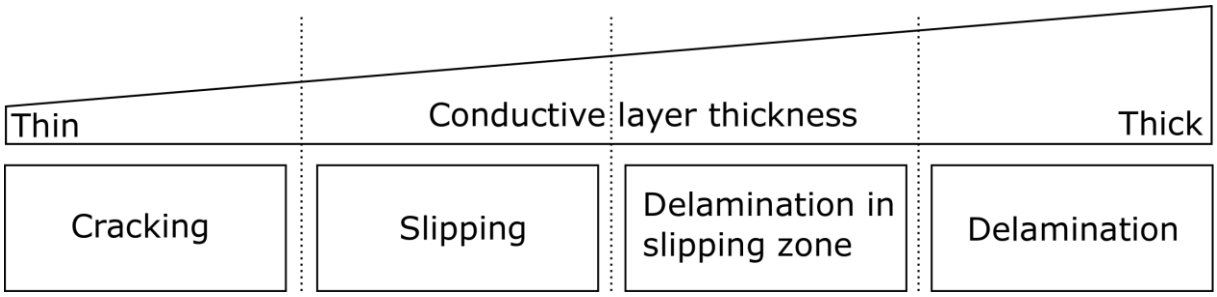

Fig. 19. Four failure modes with the conductive layer thickness.

Cracking differs from other modes based on where the failure occurred in the structure. In cracking failure, failure occurs on the conductive layer when the layer is cracked and split [40]. Cracking makes the conductive layer discontinuous, as shown in Figure 20. Cracks and splits occur mainly at curved edges and apexes if they are in the conductive layer structure [41]. The work needed for cracking, work on cohesion, can be defined in equation (18),

$$\mathrm{W}_{coh} = 2E \tag{18}$$

where E is surface energy of the material [42].

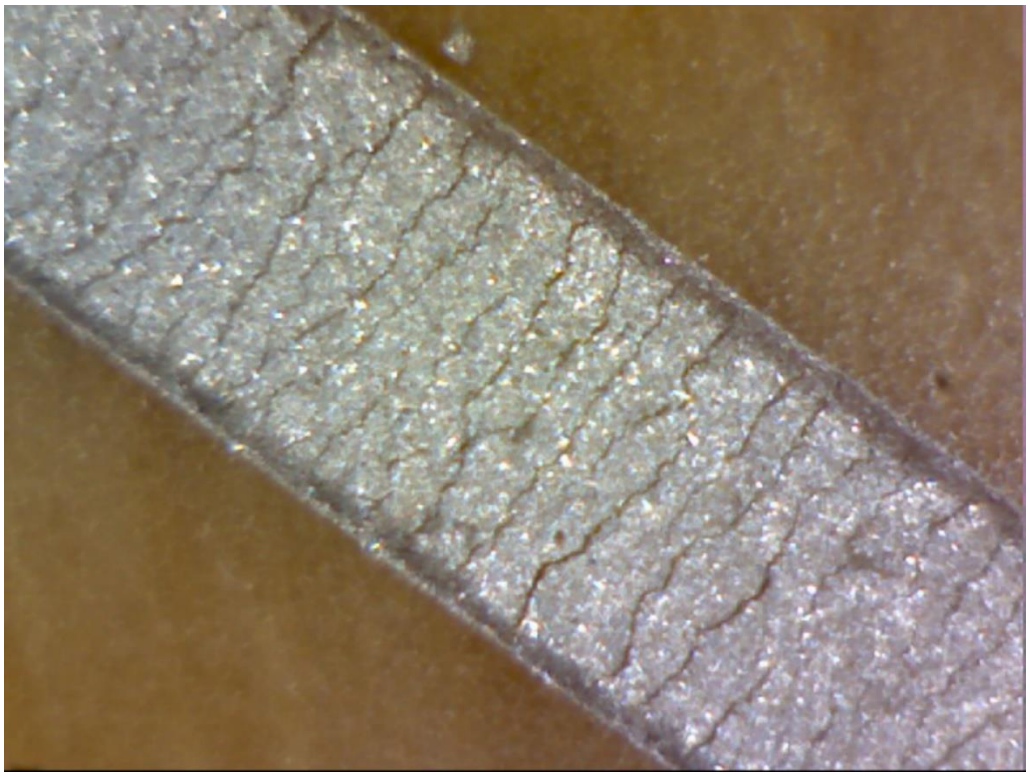

Fig. 20. Example for cracking in conductive layer.

Plastic deformations also affect the failure of the conductor. According to von Mises criteria, plastic deformation in a material begins when the shear stress is more than half the yield stress of the material. In plastic deformation, the conductor does not necessarily fail, but the material does not return to its original shape, which can cause failure. Various parameters, such as Young's modulus, elastic limit, surface energy, radius of curvature and load, affect deformation. [43]

Slipping and both delaminations occur as failures between the conductive layer and substrate interface. The work needed for slipping and delamination can be estimated through the work of the adhesion phenomenon. The work of adhesion W_{adh} for two solid materials can be defined in equation (19),

$$W_{adh} = E_1 + E_2 - E_{12} \tag{19}$$

where E_1 is the surface energy of material 1, E_2 is the surface energy of material 2 and E_{12} is surface energy of the interface of materials 1 and 2 [42,44]. In slipping, the substrate stretches more than the conductive layer and therefore, a small separation is formed as shown in Figure 21. Slipping is generally due to the fact that the adhesion between the conductive material and the substrate is not suitable and the conductive material can move on the substrate during stretching and locks during stretching and thus the structure does not recover [45]. Slipping can also expose the conductive layer to cracking or delamination in the slipping zone.

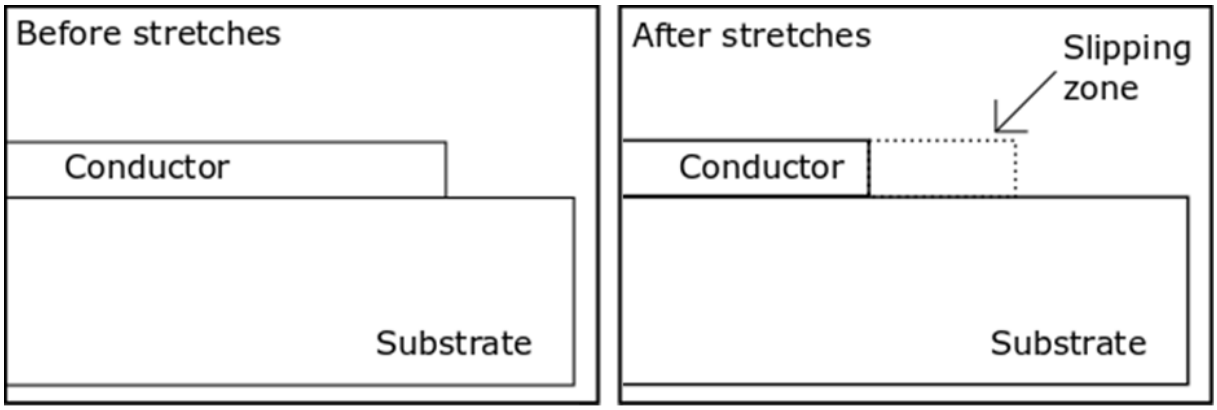

Fig. 21. Slipping zone.

Delamination can occur in the slipping zone or anywhere between the conductive layer and the substrate. In delamination, the conductive layer is detached from the substrate due to poor adhesion and stress on it. Structure of delamination can be seen in Figure 22. By improving the adhesion between the conductive layer and the substrate, we can decrease slipping and delamination failures. [40, 45]

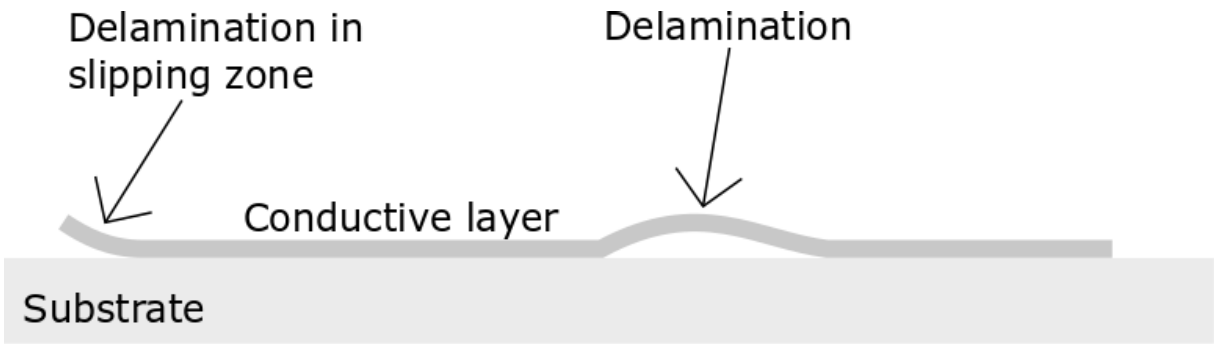

Fig. 22. Two modes of conductive layer delamination.

In printed and stretchable electronics, the electrically conductive layer, or the printed ink, contains particles of different sizes and shapes, if the conductive material was not a perfect sinter [30]. The location of these particles changes during stretching, which leads to the elongation of the electrically conductive path and possibly also the narrowing of the path. In addition, the particles may fall to pieces, sintered or adhere to each other under the stretching. As a result, the length of the electrically conductive path increases and the thinner sections of the chain formed by the particles increase the resistance. Resistance increase in the conductive layer without being perfectly sintered is shown in Figure 23. With a perfectly sintered conductive layer, the particles are sintered together, whereby the conductive layer is uniform without flakes and stretching, causing the thinning and narrowing of the conductor and increased resistance. The resistance of the non-stretched conductor is affected by percolation, the conductor material and structure, as well as the binder and solvent material and their concentration. Percolation is affected by sintering. [46, 47]

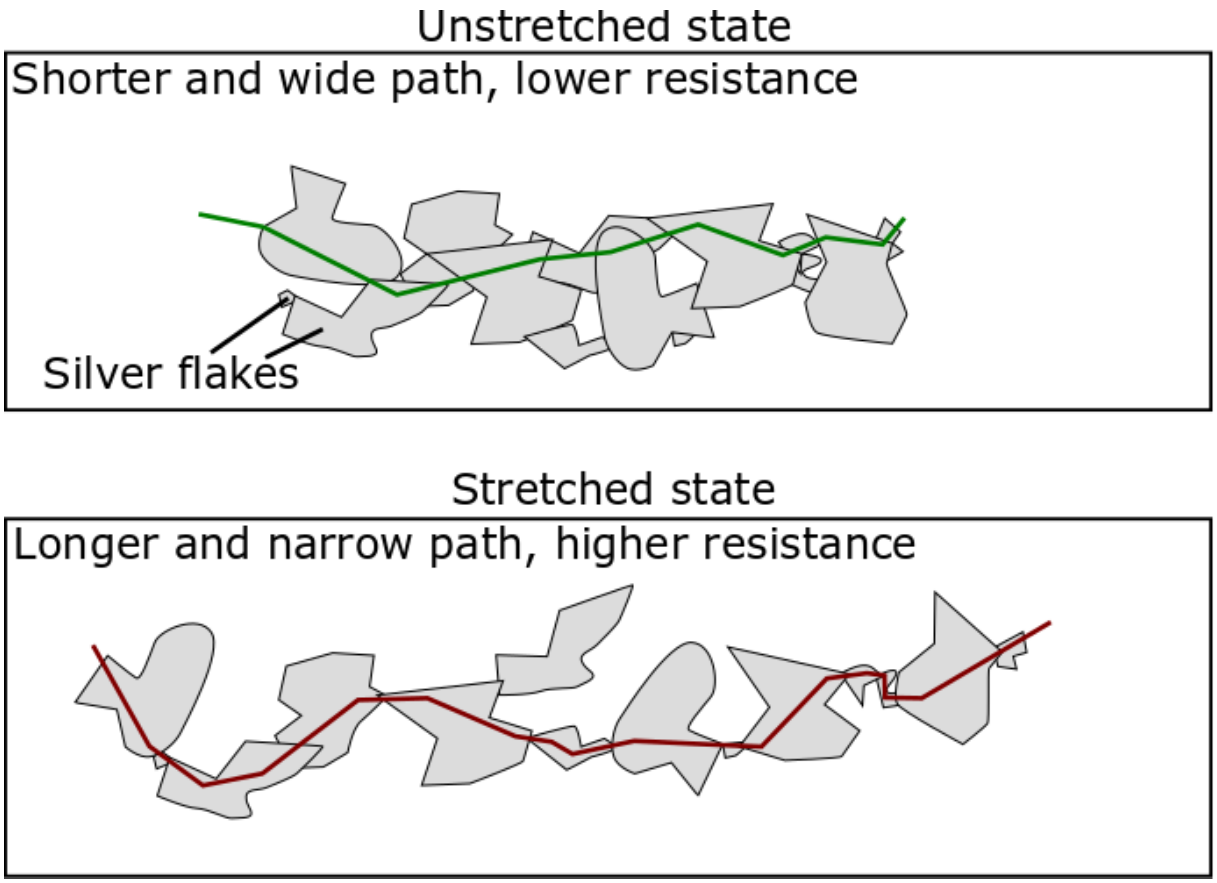

Fig. 23. The structure change impact resistance with stretched and un-stretched state [30].

When the mode of failure and the reasons for increased resistance can be specified, it is easier to locate and distinguish between the causes and therefore to improve components of the materials and manufacturing. Good, proven material choices and high-quality manufacturing methods can reduce the number of failures. Therefore, it is important to do reliability testing in product development to find the best material and manufacturing method combinations, failure modes and failure reasons, as well as limit values for resistance and useful life.

3.3 Standards

A standard is a solution to a common, well-known problem. The purpose of standards is to benefit the industry through compatible, proven and safe ways to do things. Thus, each company does not have to do all the development work itself, but can use ready, standardized manufacturing and testing methods. The purpose of standards is also to make life easier for consumers by improving product quality and compatibility. A good example of a user-friendly standardization is the print size A4, which is 210 mm wide and 297 mm high [49]. [48]

Testing standards for stretchable electronics consist mainly of standards and guidelines for the testing environment and testing equipment, but there are no standards for testing implementation except for a few tests. Standards for various stretching electronics tests are listed in Table 3. [50]

Table 3. Test standards for printed electronics flexibility and stretchability tests [50].

Test type	Test item	Applicable standard
Stretchability testing	Stretchability limit test	No known industry standard
	Cyclic stretchability test	No known industry standard
	Stretchability under constant elongation condition	No known industry standard
	Stretchability under constant torsion condition	No known industry standard
	Stretchability under cyclic torsion condition	No known industry standard
Bending testing	Variable radius bending test	IEC 62715-6-1
	Variable angle bending test	No known industry standard
	Free arc bending test	No known industry standard
	DeMattia flexibility test	ASTM D813, ASTM D430, ISO 7854
	Loop bending test	No known industry standard
	Folding endurance test	ISO 5626, IEC 62899-201
Torsion testing	Torsion test	No known industry standard
Rolling test	Rolling flex test	ASTM F2750
	Coiling flex test	No known industry standard
	Sliding plate test	No known industry standard
Crumbling test	Crease test	ASTM F2749
	Schildknecht test	ISO 7854
	Crumple flex test	ISO 7854, ASTM F392
	Vamp flex test	ISO 5402-2
	Bally flex test	ASTM D6182

In general, the standards define the exact requirements for the test conditions and the test setup. A specific 23 ° C ± 1 ° C air temperature with humidity of 50% ± 5% at ambient atmosphere is recommended for stretchability and flexibility testing of printed electronics [50]. Some test standards define slightly different test conditions to be followed in standard tests. Standards define the setup of the test device, preparations and requirements and, for example, how the test sample should be attached to the device. In addition, test sequence and limit values for test failure and success are defined in the standard. There are also detailed instructions for documenting test results. [50]

The standards used in this thesis for the stretchability limit test and cyclic stretchability test include the IPC-9204 standard guideline test sample measurement (Figure 24) and equation (20) is used to calculate stretchability,

$$\text{Stretchability} = \frac{\text{Final ink lenght} - \text{Initial ink lenght}}{\text{Initial ink lenght}} \quad (20)$$

and ASTM-D882-12 standard for test sample attachment, Figure 25. [50, 51]

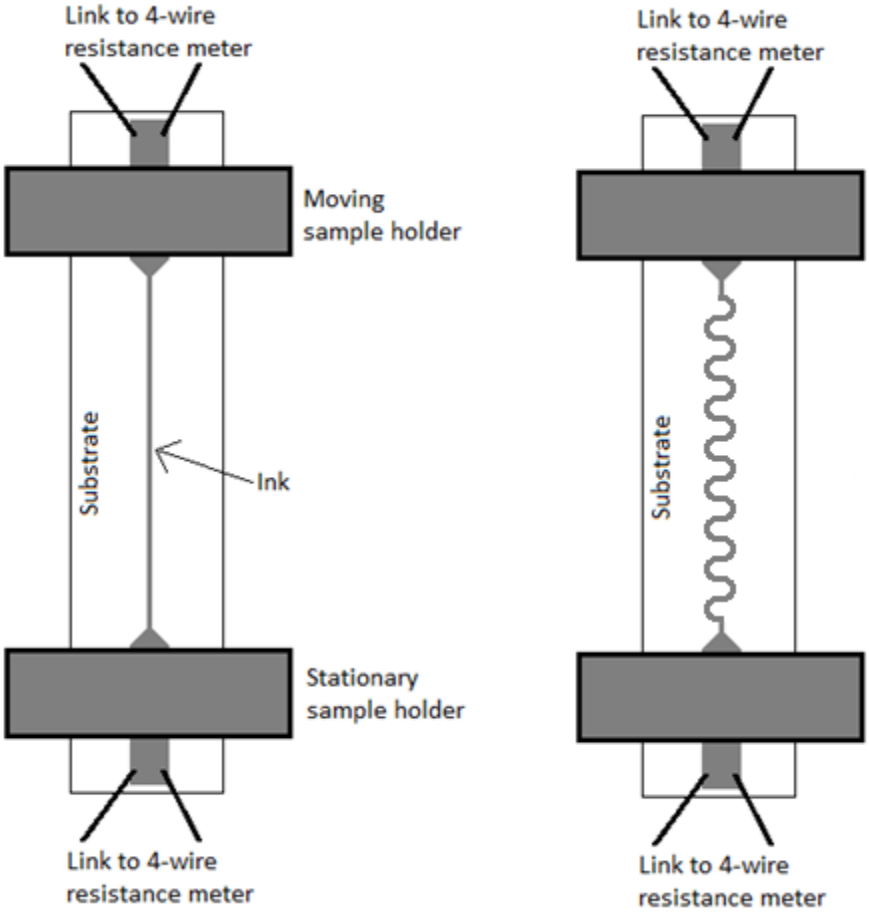

Fig. 24. Stretchability testing of printed ink samples.

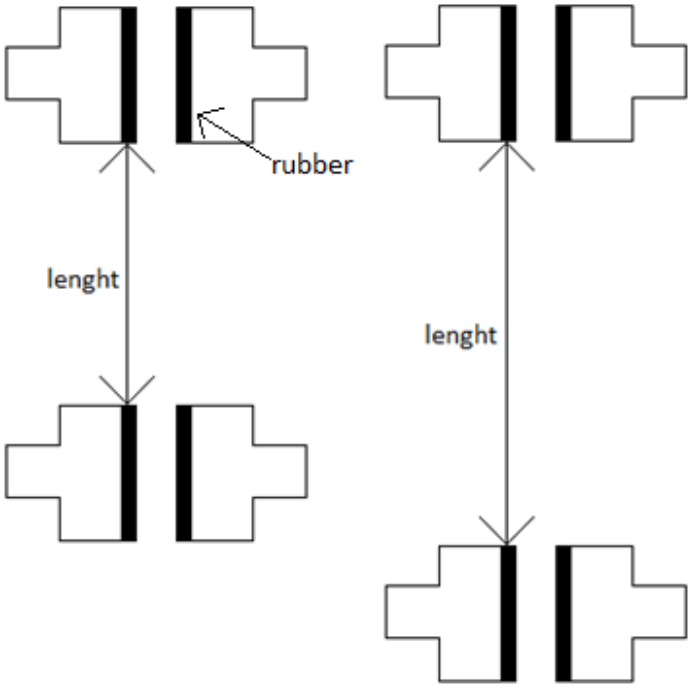

Fig. 25. Stretchability test holders.

3.4 Measuring and testing in other organizations

Since there are no clear standards for most of the tests, it is good to look at test methods of other organizations. Comparing these methods, we can find the best way to do testing for our use. In addition, other organizations' ways of reporting measurement results can be viewed. This makes it possible to show our measurement results using the same methods as other organizations and further enables direct comparisons.

For strain testing, the testing equipment is very simple. Thus, many different organizations have similar testing equipment in many ways. At its simplest, the stretching equipment is based on the self-implemented control of the Arduino development platform, but also commercial stretching equipment is used [3, 52-57]. Equipment are used both vertically and horizontally for stretching [3, 52-57]. Resistance measurement has been accomplished with a separate measuring device that measures resistance from outside the clamps as instructed in the IPC-9204 standard [3, 50, 52-57]. Typical testing equipment is shown in Figure 26. Although the stretching equipment is very simple, many organizations do not tell which devices and equipment configurations have been used to achieve the measurement results.

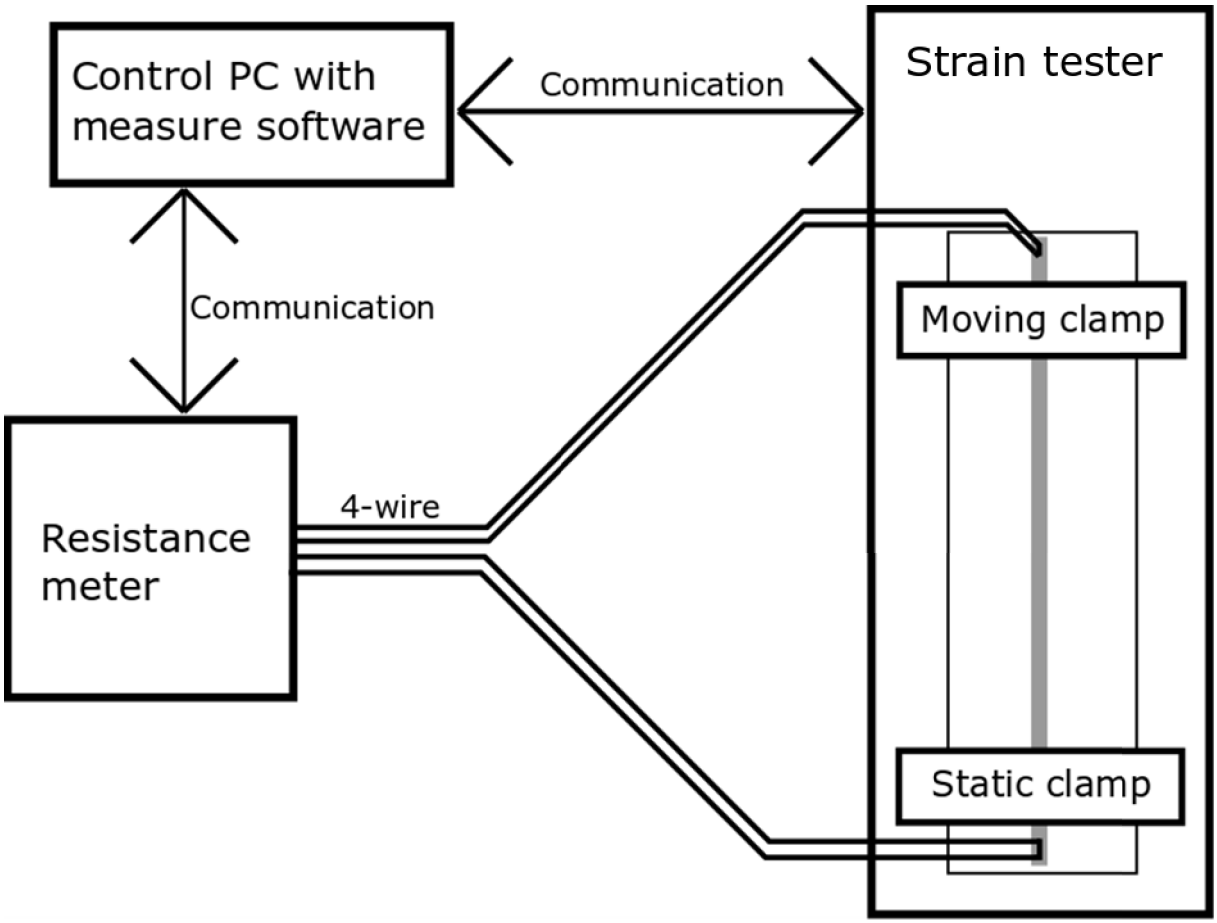

Fig. 26. Typical strain tester.

The measurement results can be presented in a few different ways and the ways to present results differ slightly in different organizations. Figure 27 shows two different ways to plotting a result curve in stretching tests. Figure 27 a) the stretch curve is plotted in reverse orientation on the horizontal axis, with the release point furthest from the origin. While in Figure 27 b) the release curve is plotted forward on the horizontal axis from the origin. The resistance and its change can also be presented in many different ways. For example, the increase of resistance can be compared with the resistance value of the starting point (Figure 27 a). Resistance can also be plotted on its own linear scale (Figure 27 b). Table 4 summarizes different organizations' ways of plotting test results.

a)

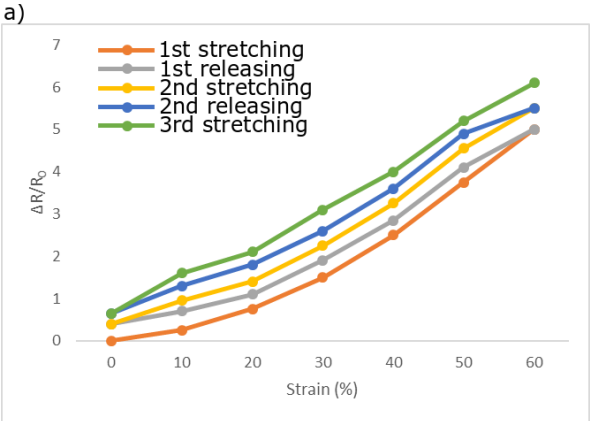

b)

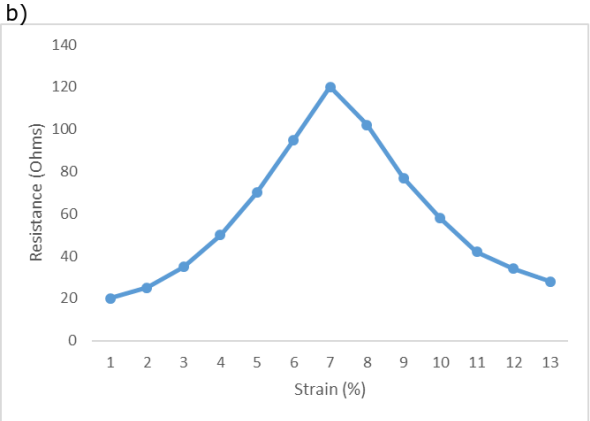

Fig. 27. Two different ways of plotting results on a graph.

Table 4. Different organizations ways to plot test result.

Reference	**Test**	**Vertical axis**	**Horizontal axis**	**Other**
[58]	Cyclic	R (Ω)	Number of cycles	
[59]	Single stretch	$\Delta R/R_0$ (%)	Strain (%)	
[54]	Single stretch	R (Ω)	Strain (%)	
[53]	Stretching and releasing	$\Delta R/R_0$ (%)	Strain (%)	Releasing is plotted backward in strain axis like fig 27 a).
[60]	Cyclic	R (Ω)	Time (sec)	
	Single stretch	R (Ω)	Strain	
	Single stretch	R (Ω)	Time (sec)	
	Stretching and releasing	R/R_0	Time (sec)	
[61]	Single stretch	R/R_0	Strain (%)	
	Cyclic	R/R_0	Number of cycles	
[62]	Single stretch	R (Ω)	Strain (%)	
	Cyclic	R (Ω)	Number of cycles	
[63]	Single stretch	$\Delta R/R_0$ (%)	Strain (%)	
[3]	Single stretch	logarithmic R (Ω)	Strain (%)	
	Three cycles	logarithmic R (Ω)	Strain (%)	Not releasing, stretches only
[56]	Single stretch	R (Ω)	Strain	
[30]	Single stretch	R (Ω)	Strain (%)	
	Stretching and releasing	R (Ω)	Strain (%)	Releasing is plotted forward in strain axis like fig 27 b).
[55]	Single stretch	R/R_0	Strain (%)	
	Cyclic	R/R_0	Number of cycles	

As seen in Table 4, the most popular way to plot results on a graph is to use linear resistance on the vertical axis. An almost as popular method is to compare the change in resistance to the resistance starting value. Strain percentage is the most commonly used unit on the horizontal axis to show results for single strain tests. In cyclic tests, the horizontal axis unit is usually number of cycles. This is certainly one of the best ways of plotting results on graphs, because usually the number of cycles or the magnitude of strain is one of the easiest ways to compare samples. Resistance shows the extent of electrical conductivity and how much it changes at every point on the horizontal axis.

4 MEASURING IN THIS THESIS

This chapter introduces the test device implemented in this thesis and what can be done with it. In addition, we review the test results obtained, and we compare how different manufacturing techniques, materials and different shapes of conductors affect the duration and resistance of the sample. The reliability of the selected sample combination in the cyclic test is also tested

4.1 Device and setup

The main target group for the measurements with the device is printed samples of stretchable electronics. The test device is used for strain testing and it measures force, distance and resistance of the sample. These values should be able to measure the device at each step of the measurement and finally save the file for later review.

The test device was built using the Mark-10 ESM303 tension test stand as the base. The ESM303 has a control panel that can be used to control the device to make various stretches. The tester can be used to perform strain tests from individual stretches up to 99999 cycles and the top and bottom positions of the cycles can be set to 0–9999.9 seconds dwell time. The device is capable of stretching at a speed of 13–330 mm/min, at a resolution of 0.02 mm and an accuracy of ± 0.05 mm per 250 mm. The device shows the stretched distance on the control panel screen, but it can also be read on the computer via USB communication. [64]

The force is measured by the Mark-10 Series 7 digital force gauge attached to the ESM303 test stand. Communication between test stand and digital force gauge has been implemented with an RS-232 communication cable. In this case, the force from the force gauge can be read through same USB interface than travel value. In VTT, two different force gauges can be used in the measurement with a maximum force of 50 Newtons with 0.01 resolution or 500 Newton with 0.1 resolution. The accuracy of the force gauges is ± 0.1% of full scale. Force gauges with different maximum force are also available from the manufacturer. [64, 65]

Resistance measurement is done with an HP 34401A multimeter. The multimeter can be read and controlled via computer using an RS-232 or IEEE-488 interface. This thesis configuration uses RS-232 communication. The resolution for resistance measurement is a maximum of 100 μΩ at a minimum of 100 Ω range. Maximal range is 100 MΩ. The accuracy is between 0.006 % and 0.81 % depending on the used range and environmental conditions. Resistance is measured as a 4-wire measurement. [66]

A LabVIEW-implemented program is used to communicate with devices from a computer. The communication between the devices is illustrated in Figure 28. The program communicates with the multimeter and test stand via the COM ports of the computer. When the operator started the measurement, the program initializes the connections and then sends commands to the multimeter for reading the 4-wire resistance, as well as a test for reading the power and distance. After sending, the program reads the received data from COM ports and plots them in real time in the program interface. The program interface is shown in Figure 29. In addition, the program collects the data in a table along with the time parameter, and after the measurement is completed, the data is saved in a text file, as well as in an excel table. Appendix 1 is an example of a test text file. The range of the multimeter can be adjusted from the program. If the measured resistance is higher than the range and the multimeter indicates overload, it is also marked in the text and excel files.

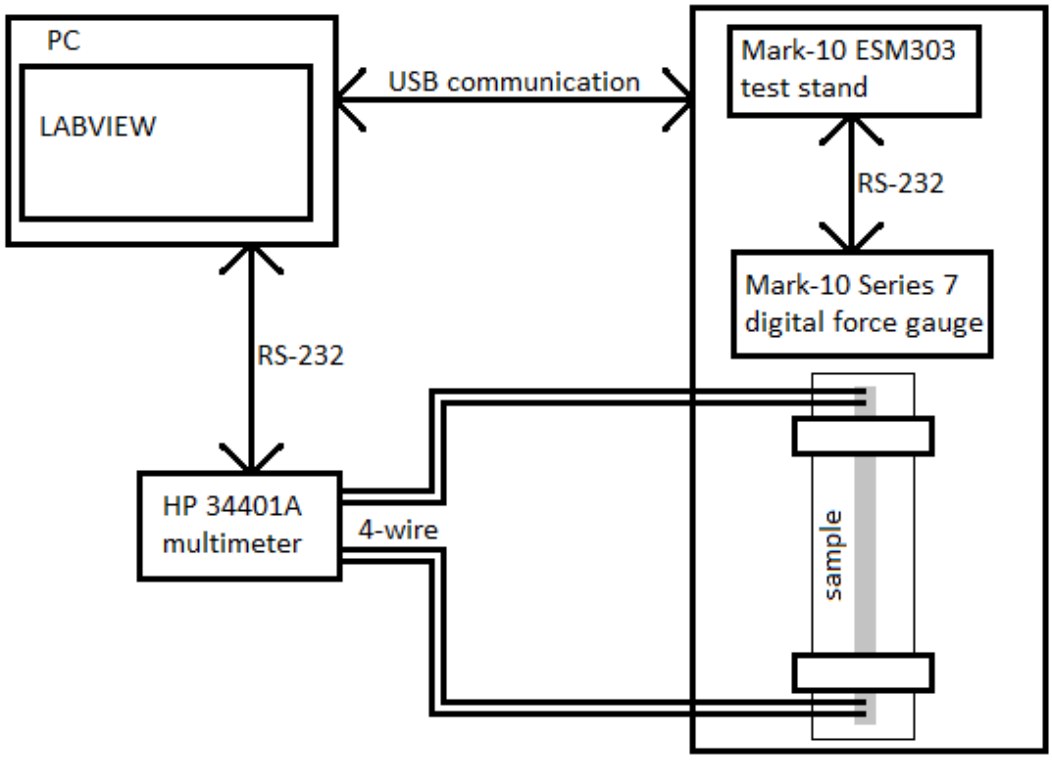

Fig. 28. Diagram of strain test device setup.

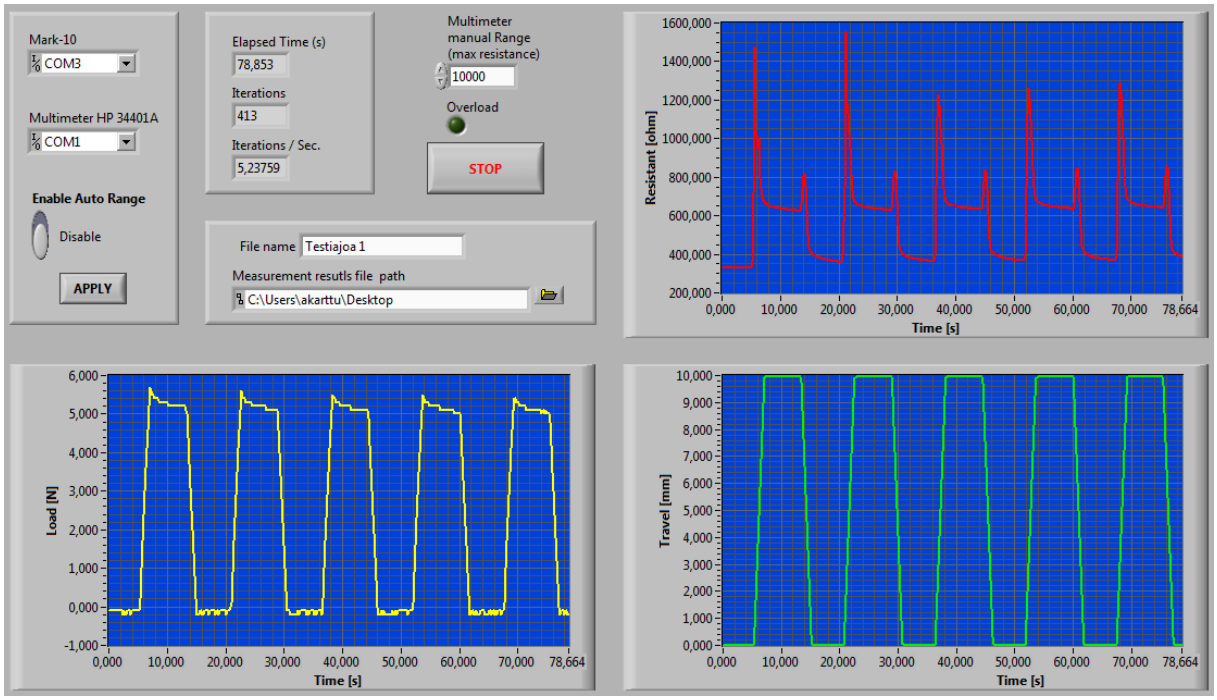

Fig. 29. LabVIEW program user interface of the strain tester.

Attachment of the test sample to the test device is implemented in accordance with the standards IPC-9204 and ASTM-D882-12. The clamps attached to the sample of the stretching tester are coated with rubber in accordance with ASTM-D882-12 so as not to damage the conductive layer of the sample. The resistance measurement attachment is made outside the

strain area in accordance with IPC-9204 to avoid stretching changes in the multimeter contacts. The attachment of the sample to the test device is shown in Figure 30.

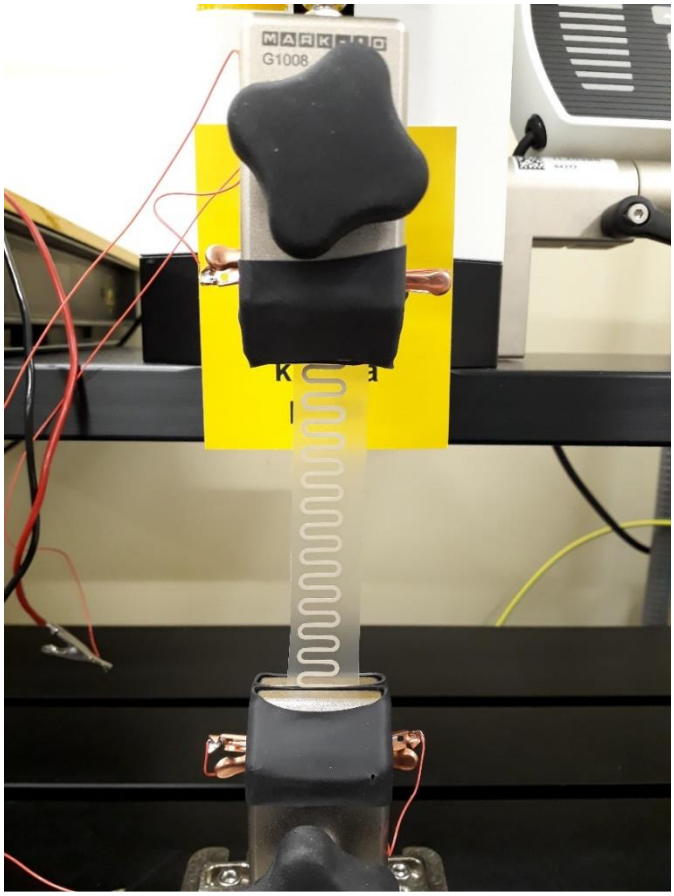

Fig. 30. The attachment of a sample.

The test equipment has been placed in stable environmental conditions in the clean room. The temperature in the clean room is 21 °C (+/- 1 °C) and humidity is 45 % (+/- 10 %). Although the temperature and humidity are slightly lower than those specified in the standards, test devices are in stable and unchanged environmental conditions. Therefore, environmental conditions do not cause variability in the test results. The whole test setup is shown in Figure 31.

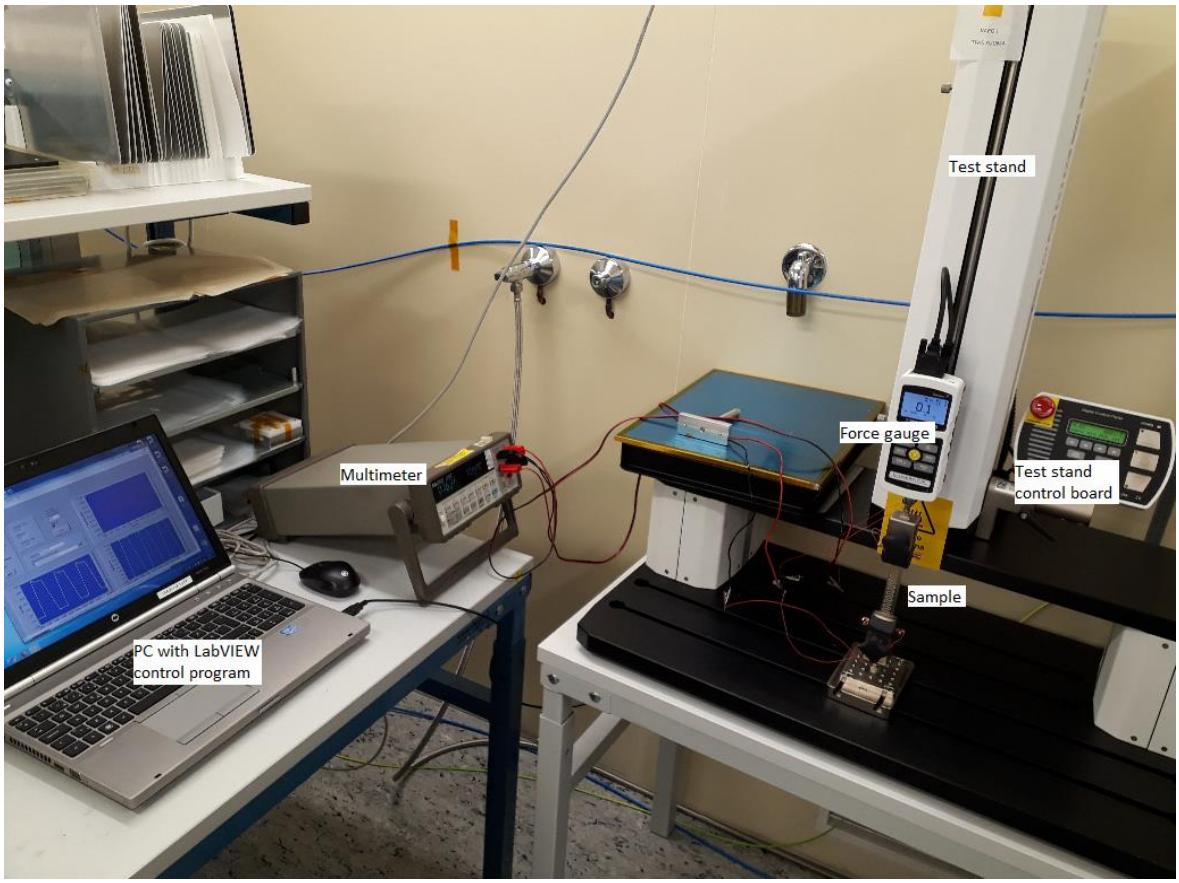

Fig. 31. Test setup.

The test device is suitable for all types of strain measurements where the sample is straight or twisted. When twisted, the sample mounts must be locked in the desired position manually before the measurement is started and the twist during measurement cannot be changed. The device can be used to perform both one-time stretchability limit tests as well as cyclic tests.

4.2 First measurements with the test device

The test plan of the first measurements was made for the stretchability limit tests. Test plan was based on standards and experiences from previous measurements. The test plan is shown in Table 5.

Table 5. Test plan for the stretchability limit test.

Stretchability limit test	Description
What is measured	Sample force, sample elongation, and sample resistance at the start and during the test are measured in the sample.
Test conditions	The temperature of the measurement environment is 21 °C (+/- 1 °C) and humidity 45 % (+/- 10 %) at atmospheric pressure.
Prepare for the test and progress	Stretching with the test device is started by attaching the sample to the device so that the sample is in a straight, unstretched state. The sample is stretched only once and

	data is measured during this time.
Ending the test	Stopping the stretching when the electrical conductivity of the sample is interrupted or the resistance increases above the agreed value. In this work, a limit of 1000 Ω is used.

In the first measurements, samples printed with silver paste on the TPU substrate are tested. Samples are made via the screen printing technique. The following were compared: the effect of substrate thickness, different silver pastes, screen print direction and drying on sample reliability and strain resistance. In addition, different wire patterns are compared.

There are a total of 26 tested sample combinations or test points, with a total of five inks and three different substrate thicknesses. Five different temperature and time combinations are used as dry methods, plus one method with a UV heater. The silver pastes, substrates and drying used in test points are listed in Table 6. Each test point has nine test samples. Samples include four different wire patterns vertically and horizontally printed and one full-filled sample (full in Figure 32). Other wire patterns are horseshoe (AH and AV in Figure 32), U-shape (BH, BV), pulse (CH, CV) and single line (DH, DV). The line width of the printed wire is 1.0 mm and the width of the full-filled strip is 20 mm. The length of the wire patterns without stretching is 105 mm with pads. Each sample is stretched 70 mm from the center of the sample. Samples of each test point are printed on one sheet as shown in Figure 32. Samples are cut off for testing along the lines surrounding the sample.

Table 6. Various silver pastes, substrates and drying conditions of test samples.

Silver pastes		Solid	Binder	Solvent
	Manufacturer 1	Silver (66.6 %)	Unknown	Unknown
	Manufacturer 2	Silver (80-90 %)	Siloxane polymer (10-20 %)	2-(2-butoxyethoxy) ethanol (DEGBE) (1-5 %)
	Manufacturer 3	Silver (55-65 %)	Polymer resin (5-13 %)	Dipropylene glycol monobutyl ether (28-45 %)
	Manufacturer 4	Silver powder (62.8 %)	Polyester (14.5 %)	Ethyl carbitol acetate (22.7 %)
	Manufacturer 5	Silver flake (50-60 %)	Maleic acid terpolymer with vinyl chloride and vinyl acetate (1-5 %)	Diethylene glycol ethyl ether acetate (30-40 %)
Substrates	TPU-50 µm			
	TPU-100 µm			
	TPU-150 µm			
Drying conditions	120°C - 30 min			
	140°C - 10 min			
	140°C - 30 min			
	160°C - 10 min			

	160°C - 30 min
	UV 1000W - 30 s + 140°C - 30 min

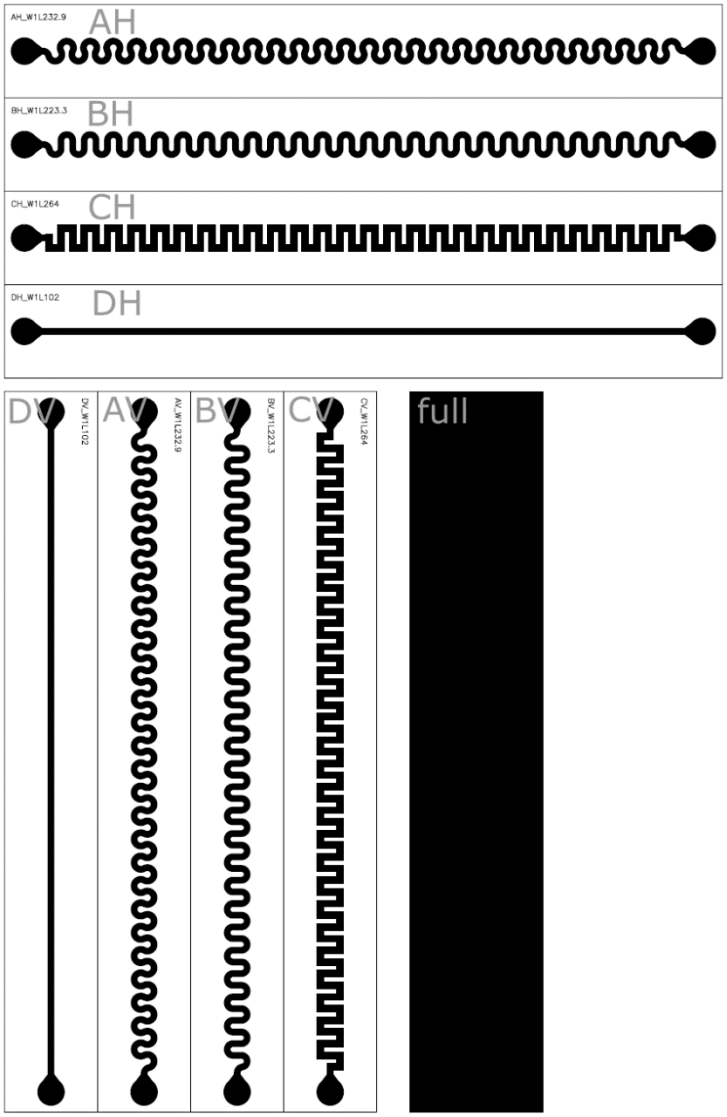

Fig. 32. Layout of test point and its test samples.

4.3 First measurement results

In the processing of the measurement results, the focus was on finding out the differences between five categories, between the pastes, between the substrates, effect of wire pattern, differences between horizontal and vertical screen printed samples and differences between drying methods. Differences were checked with the initial resistance and maximum stretch. The initial resistance (R_0) was determined from the mean of the measured values before stretching. The maximal strain was the value at which the increase of resistance is still steady. If the resistance (R) increased steadily to 1000 Ω, the last value less than 1000 Ω was used as

the maximum stretch. To determine stable increase of resistance, the derivative of the resistance-strain curve was used according to equation (21),

$$\frac{\partial R}{\partial \epsilon} > 35 \tag{21}$$

where $\partial\epsilon$ is a derivate of strain in percentage points. In other words, the increase of resistance is considered to be stable if it increases by a maximum of 35 Ω during one percent strain or 50 Ω during one millimeter strain. Examples of steady increase of resistance and determination of maximum strain in figures 33 and 34. Appendix 2 shows stable resistance-elongation graphs for all samples tested. In the table in Appendix 3, the maximum strain of all samples and the mean of maximum strain of the test point are tabulated. Initial resistances are in Appendix 4.

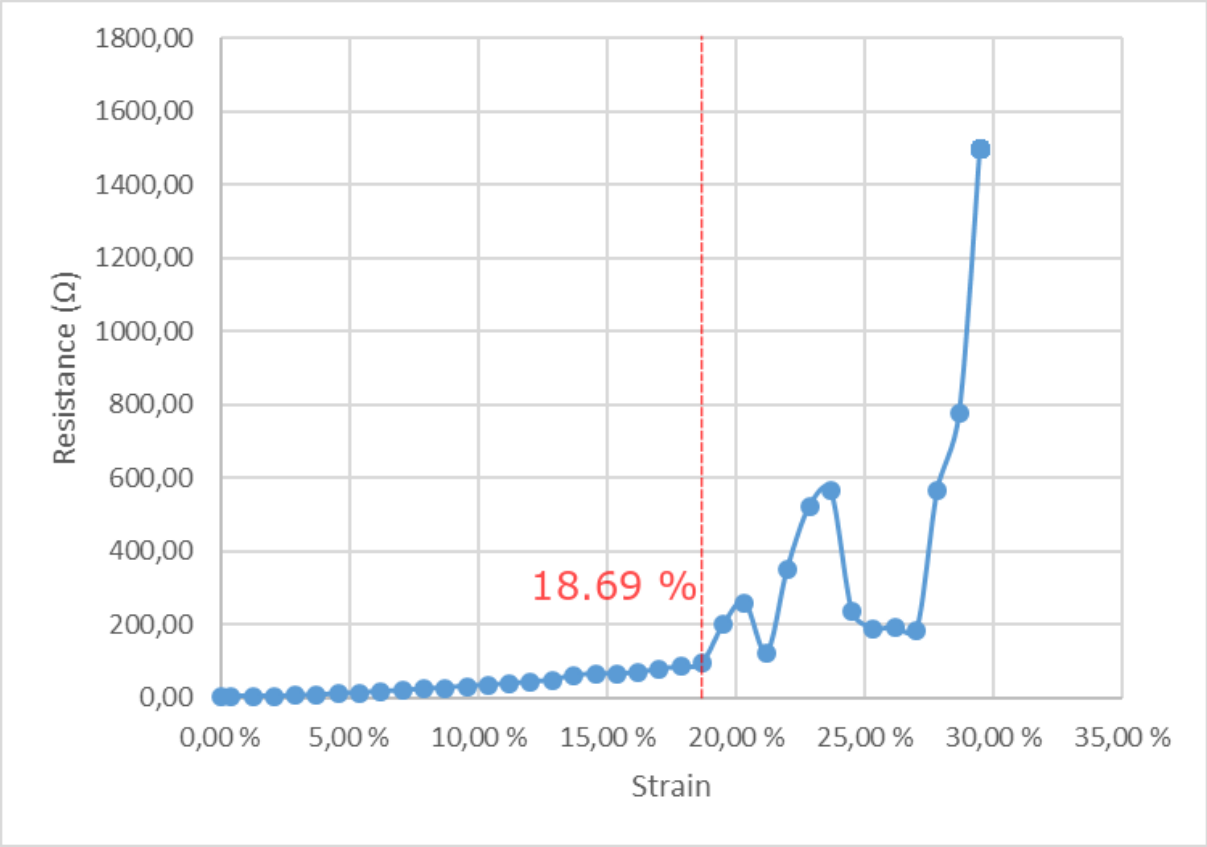

Fig. 33. Example of max strain selection, resistance-strain curve.

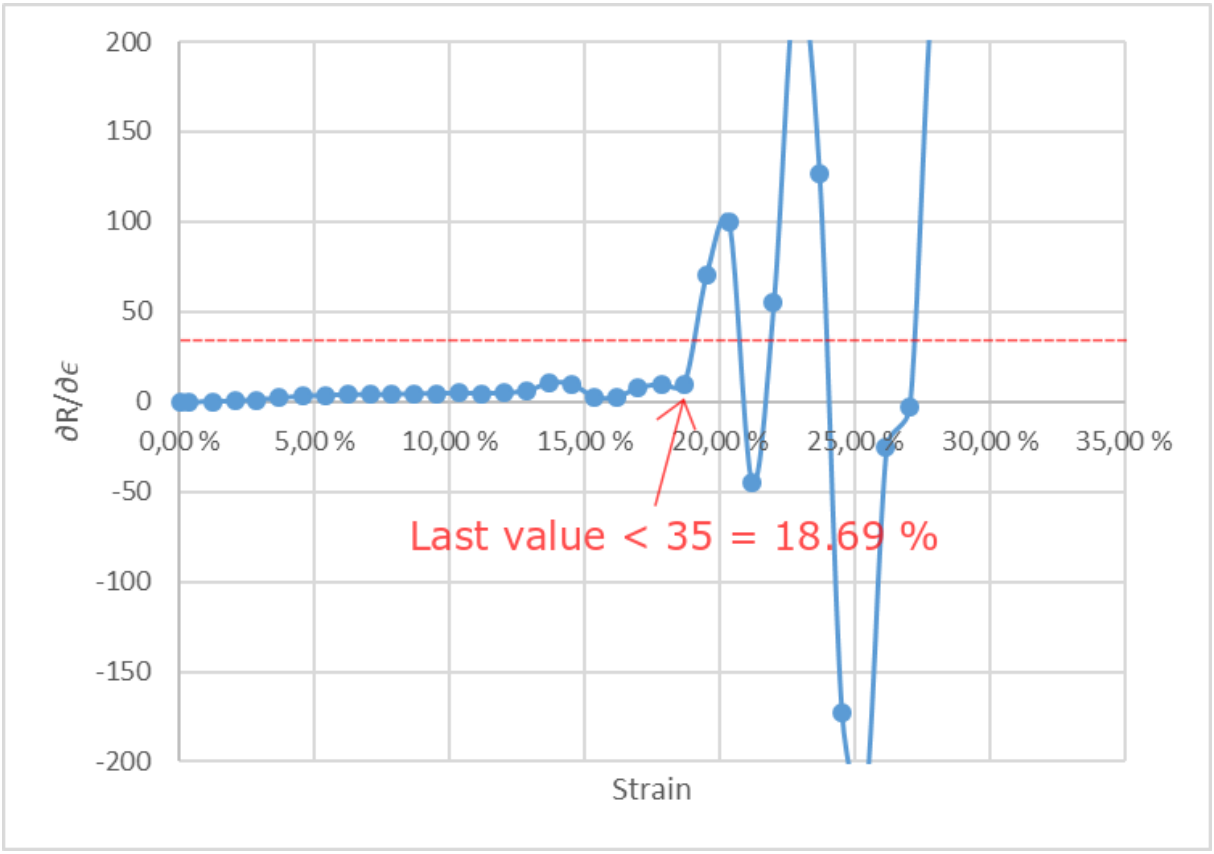

Fig. 34. Derivate of Figure 33 resistance-strain curve with strain.

The differences between the manufacturer's pastes can be viewed in two different methods: examining the initial resistance and maximum strain averages of samples printed with paste. Another way is to look at the median of the measurement results of samples printed with paste, whereby the effect of the worst and best samples on the result is not so great. The results from both methods, as well as minimum and maximum values, are tabulated in Table 7. The table shows that the values of the test samples differs significantly from some manufacturer's pastes.

Table 7. Measurements results between different manufacturers pastes.

	Number of samples (from test points)	Average		Median		Min/Max	
		R_0	Max strain	R_0	Max strain	R_0	Max strain (%)
Manufacturer 1	9 (1)	12.01	117.58 %	14.73	114.37 %	0.46/16.82	93.06/159.20
Manufacturer 2	72 (8)	3.67	53.18 %	4.42	26.44 %	0.09/5.89	4.00/207.29
Manufacturer 3	9 (1)	15.31	47.54 %	18.52	47.51 %	0.61/20.75	39.34/54.77
Manufacturer 4	72 (8)	3.80	56.10 %	4.08	40.73 %	0.10/6.28	2.86/224.26
Manufacturer 5	72 (8)	5.70	68.21 %	7.08	55.86 %	0.18/5.89	14.06/195.43

Each ink has a different silver content, shape and particle size distribution, as well as binder and solvent material and their concentrations. The low initial resistance of manufacturer 2 and 4 pastes can be explained by a thicker conductive layer thickness. The average of each manufacturer's samples conductive layer thicknesses, sheet resistance and volume resistivity are shown in Table 8. With all samples the same printing mesh has been used, so differences in layer thicknesses are mainly due to the properties of the pastes, such as viscosity, surface tension and solvent to binder ratio. High initial resistance of the manufacturer 1 and 3 pastes can be partly justified by the thin layer thickness, but the relatively low initial resistance of manufacturer 5 paste to thin layer thickness is due to other factors, such as good conductivity. This is also seen by the fact that the manufacturer 5 samples have the best volume resistivity. Manufacturer 5 paste has very uniform quality of strain durability and although the paste has been tested with a large sample size, there were no particularly weak samples that were seen from the minimum strain value. The high 30–40 % solvent content of the paste of manufacturer 5, combined with the extensive drying times and temperatures suitable for it, can be a part of the good strain durability of the sample. There was a large variation between the samples of manufacturer 2 paste, partly explained by the low 1–5 % solvent content. In some samples, the solvent is believed to have evaporated too much, resulting in a very good initial resistance, but poor strain resistance, and poor adhesion between the ink and the substrate. Due to the effect of the hardened conductor and the thick layer thickness in some of the samples of the manufacturer 2 paste, delamination during stretching occurred. Delaminated sample shown in Figure 35.

Table 8. Average of samples conductive layer thicknesses from different paste manufacturers.

	Number of samples (from test points)	Test points (number of samples)	Average thickness (µm)	Average sheet resistance of unstretched samples (mΩ/□)	Average volume resistivity of unstretched samples (Ω·cm)
Manufacturer 1	9 (1)	1 (9)	5.08	69.69	3.54E-05
Manufacturer 2	72 (8)	8 (72)	21.17	20.09	4.25E-05
Manufacturer 3	9 (1)	1 (9)	3.81	90.05	3.43E-05
Manufacturer 4	72 (8)	8 (72)	13.61	20.93	2.85E-05
Manufacturer 5	72 (8)	8 (72)	6.00	33.22	1.99E-05

Fig. 35. Delaminated sample with manufacturer 2 paste.

When looking at the effect of substrate thickness on the initial resistance and strain of the sample, only test points with the same pastes and same drying times for comparison should be

selected. Comparing substrate thickness, there are three test points for every thickness. Test points are manufacturers 2, 4 and 5 pastes with 160 °C 30 minutes drying. Measurement results with every substrate thickness are tabulated in Table 9. As the table shows, the thicker the substrate, the better the sample will withstand stretching. Also, the difference between average and median values decreases with a 150-µm-thick substrate compared to thinner substrates. 150 µm substrate will better take the force exerted on the sample and the sample have to be stretched with greater force. Figure 36 shows one sample stretching-force curves on different substrate thicknesses with same paste, drying condition and line shape.

Table 9. Measurement results between different substrate thicknesses.

Substrate	Number of samples (from test points)	Average		Median		Min/max	
		R_0	Max strain	R_0	Max strain	R_0	Max strain (%)
TPU-50 µm	27 (3)	3.60	34.13 %	3.41	16.17 %	0.10/6.29	2.86/160.89
TPU-100 µm	27 (3)	4.32	45.18 %	4.25	26.44 %	0.11/8.10	11.43/182.26
TPU-150 µm	27 (3)	4.52	72.94 %	4.08	67.40 %	0.11/8.37	23.80/204.14

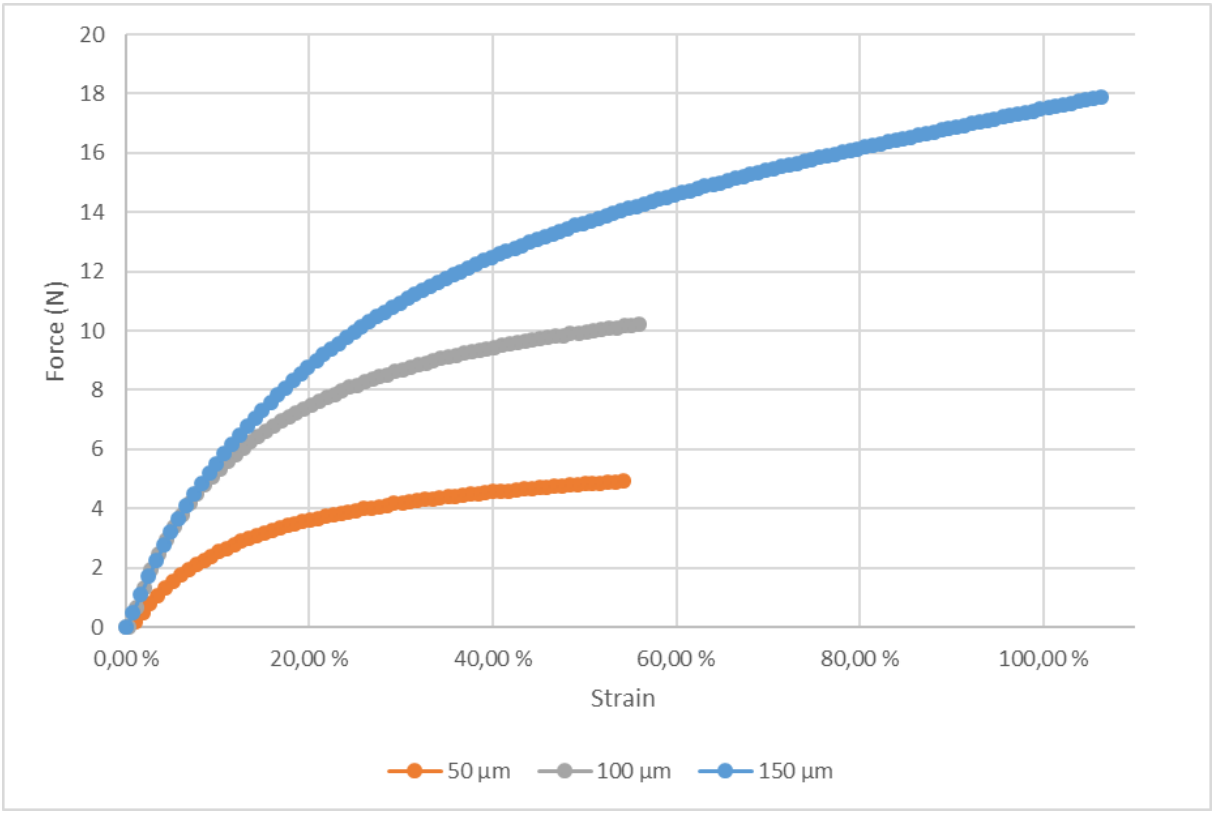

Fig. 36. Stretching force between different substrate thicknesses.

Comparing drying temperature and times, three test points are used for every drying method. Test points are manufacturer 2, 4 and 5 pastes with a 100 µm TPU substrate. The effect of drying method on the strain resistance of the sample is shown in Table 10. As shown

in Table 10, variation between different drying times and methods is very high. However, the table shows that the differences in the initial resistances of these samples were minimal and the best average, median and min/max results at maximum strain were obtained at 140 ° C for 10 minutes with the dried samples. This can be explained by the more optimal binder to solvent ratio, whereby the durability of stretching is better, although the short drying times in the initial resistor are weaker with higher solvent concentration. A short additional drying with a UV heater did not cause a significant change in the sample compared to the same drying time without the UV heater.

Table 10. Measurements results between different drying conditions.

Drying method	Number of samples (from test points)	Average		Median		Min/Max	
		R_0	Max strain	R_0	Max strain	R_0	Max strain (%)
120 °C - 30 min	27 (3)	4.47	60.65 %	4.40	50.57 %	0.10/7.25	11.26/224.26
140 °C - 10 min	27 (3)	4.60	94.06 %	5.04	81.37 %	0.11/7.81	24.54/212.89
140 °C - 30 min	27 (3)	4.31	50.20 %	4.56	37.17 %	0.09/8.10	7.89/177.14
160 °C - 10 min	27 (3)	4.65	65.99 %	5.03	54.91 %	0.12/8.02	16.14/202.00
160 °C - 30 min	27 (3)	4.32	45.18 %	4.25	26.40 %	0.11/8.10	11.43/182.26
UV 1000 W - 30 s + 140 °C - 30 min	27 (3)	4.65	50.16 %	4.61	39.00 %	0.09/8.05	4.00/198.14

The effect of the printing direction on the resistance and maximum strain of the sample is examined because the inks contain small particles. The arrangement of these particles in the sample may differ slightly depending on the printing direction of the flooding plate, which may affect the strain durability or resistance. The horizontal sample is parallel to the flooding plate. Meanwhile, the vertical sample is parallel to the direction of travel of the flooding plate. The measurement results are shown in Table 11. The results include vertical and horizontal print patterns for all 26 test points, i.e., the total of 208 samples is measured, 104 per vertical and 104 per horizontal direction. As can be seen from the results, the differences between the printing directions are very small, especially for the initial resistance. However, the elongation of the horizontally printed pattern is 6.4% or 7.6% better, depending on whether the median or average of the results is compared.

Table 11. Measurements results between horizontal and vertical samples.

	Number of samples (from test points)	Average		Median		Min/Max	
		R_0	Max strain	R_0	Max strain	R_0	Max strain (%)
Horizontal	104 (26)	5.76	49.25 %	4.96	46.51 %	1.63/20.19	2.86/131.66
Vertical	104 (26)	5.68	46.27 %	4.73	43.21 %	1.53/20.75	4.00/146.63

Different combinations of wire patterns have a combined impact on initial resistance and maximal stretch. The differences are shown in Table 12. As we can see, the Horseshoe, U-shape and Pulse shapes are worse in their initial resistance compared to the single line shape. All three winding shapes are better with maximum strain than the single line; the more rounded Horseshoe and U-shape are even better than angular pulse shape. However, the very wide full-filled sample is significantly better in terms of initial resistance and maximum strain than the other samples.

Table 12. Measurements results between different conductive line shapes.

	Number of samples (from test points)	Average		Median		Min/Max	
		R_0	Max strain	R_0	Max strain	R_0	Max strain (%)
Horseshoe	52 (26)	6,70	51,44 %	5,55	51,26 %	3.39/20.75	7.89/146.63
U-shape	52 (26)	6,32	54,55 %	5,27	51,09 %	3.22/19.41	11.31/131.11
Pulse	52 (26)	6,61	47,45 %	5,49	44,49 %	3.27/20.19	8.34/138.91
Single line	52 (26)	3,25	37,61 %	2,64	36,29 %	1.53/11.54	2.86/113.43
Full-filled strip	26 (26)	0,19	166,58 %	0,15	170,73 %	0.09/0.61	54.77/224.26

In winding patterns, a higher initial resistance is due to a longer conductor line because of winding shape. In stretching, winding of the conductor divides stretching load into a larger area, whereby the winding conductor shape can withstand greater stretching. In a single line of same thickness, load is evenly spread over the entire line, but higher because shape does not divide it into a larger area. Figure 37 shows pulse and single line microscope images with and without stretching. The figure shows occurrence of cracks in stretching. A greater strain is formed at the corners of the pulse compared to the circular shapes in the horseshoe and U-shapes, resulting in a slightly weaker maximum stretch. The superiority of the full-filled sample is based on a wide line width, whereby when the conductive layer is cracked in stretching, the cracks do not cover the line width easily and a suitable conductive path can be found. Figure 38 shows a microscopic view of the full-filled sample with stretched and unstretched state. Figure 39 shows the sample in unstretched and stretched state in the strain device.

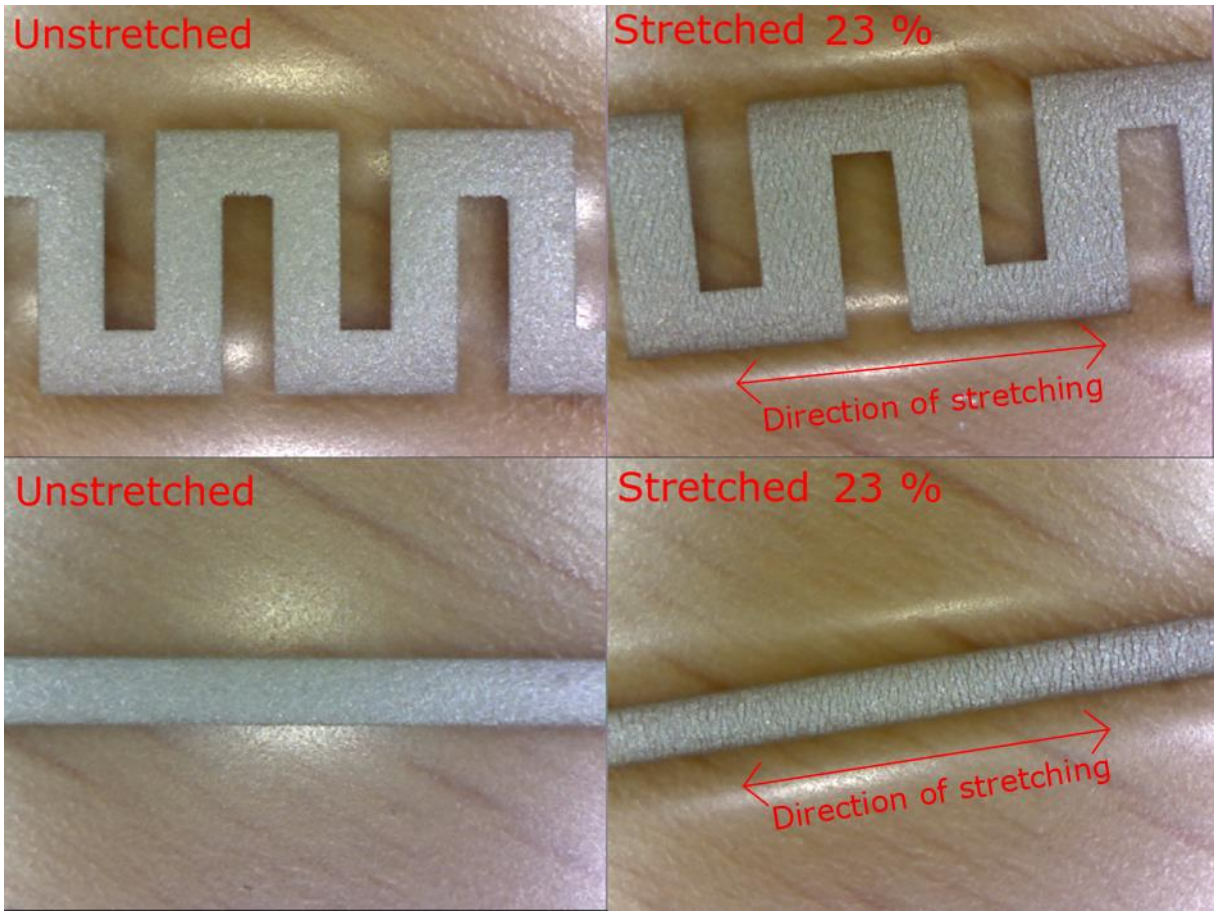

Fig 37. Microscope image of pulse and single line samples with unstretched and 23 % stretched state. Unstretched line width is 1000 µm.

Fig. 38. Microscope image of full-filled sample at unstretched and 20 % stretched state.

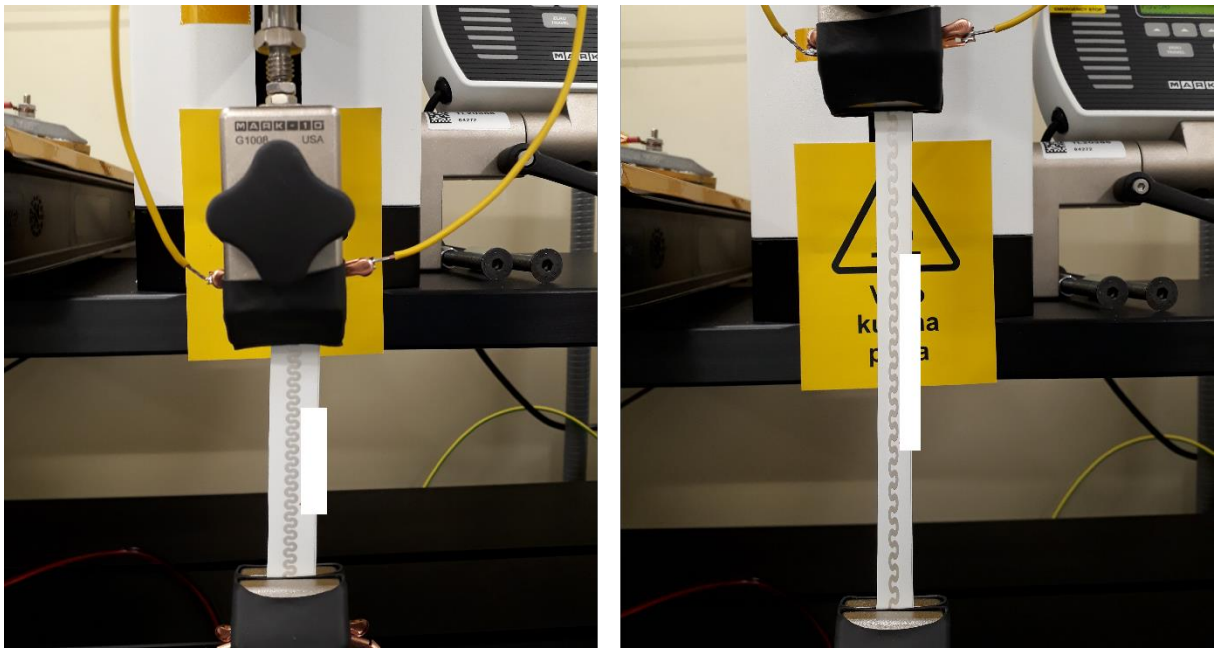

Fig. 39. Unstretched and 107.8 % stretched state of the sample.

4.4 Second measurements

The test plan for the second measurements was based on standards and experiences from previous measurements. The measurement is a cyclic stretchability test and the test plan is shown in Table 13.

Table 13. The test plan for the cyclic stretchability test.

Cyclic stretchability test	Description
What is measured	Sample force, sample elongation, and sample resistance at the start and during the test are measured in the sample.
Test conditions	The temperature of the measurement environment is 21 °C (+/- 1 °C) and humidity 45 % (+/- 10 %) at atmospheric pressure.
Prepare for the test and progress	Stretching with the test device is started by attaching the sample to the device so that the sample is in a straight, unstretched state. The samples are stretched 300 cycles without holding times. The sample was stretched 20 % at 900 mm/min.
Ending the test	Stopping cycles when 300 cycles are done or the electrical conductivity of the sample is interrupted or the resistance increases above the agreed value. In this work, a limit of 1000 Ω is used.

Samples of the second measurement are made by the roll-to-roll fabrication technique. Based on the results of the first measurement, second measurements were selected manufacturer 5 ink with the thickest 150 µm TPU substrate. Manufacturer 5 ink gave the most steady results in the first measurement. Drying of the samples is done in four 140 °C furnaces

at a speed of 2 m/min. Extra drying is also done in four 140 °C furnaces at 3 m/min. A horizontal U-shape wire pattern had the best results in the first measurement, so it was chosen for the second measurements. Wire width was the same (1000 µm) as in the first measurements. The measurement was performed on 10 identical samples. The sample with unstretched and 20 % stretched state in the strain tester is shown in Figure 40.

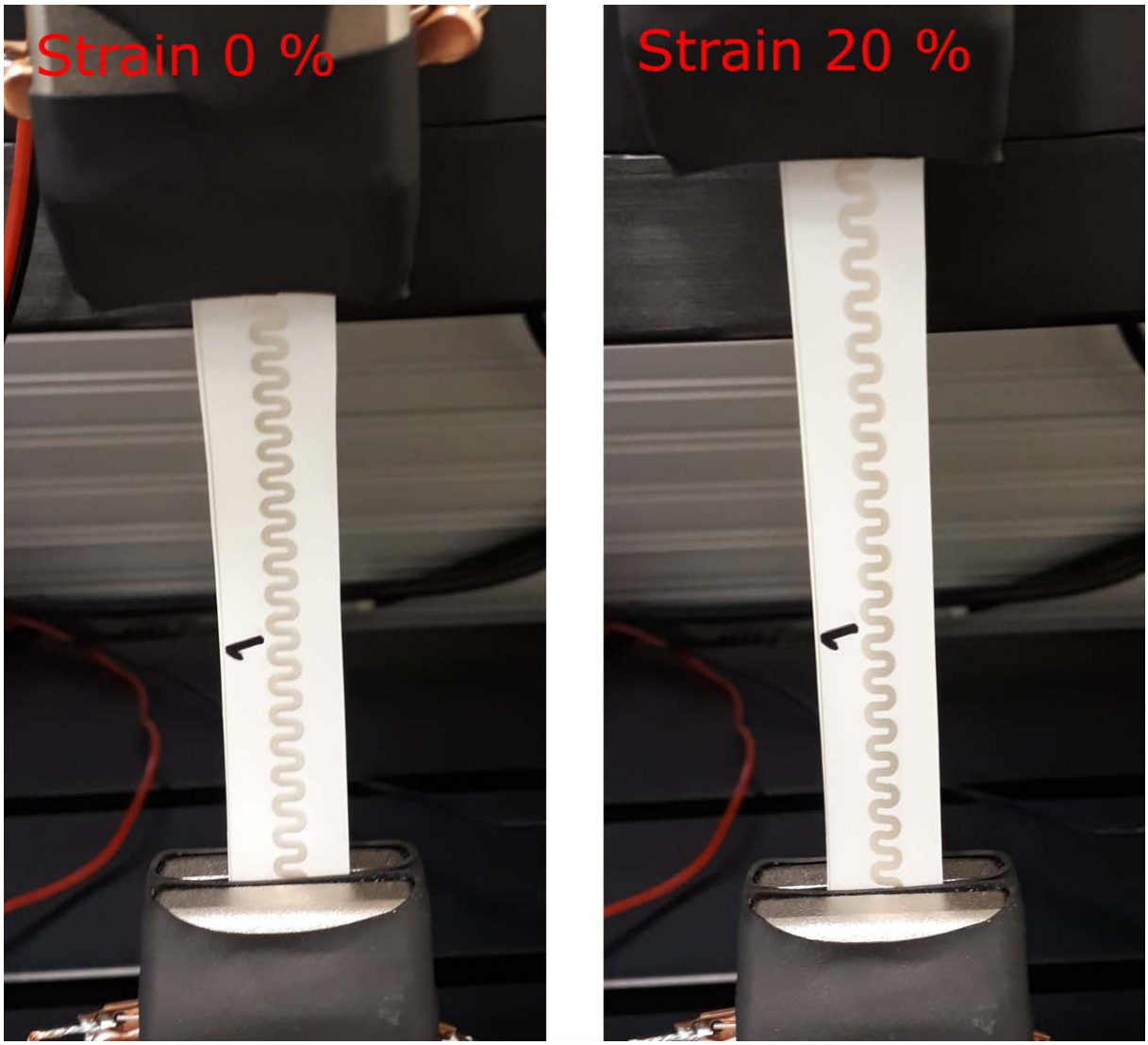

Fig. 40. Sample of cyclic stretchability test in strain tester.

4.5 Second measurement results

In the processing of the second measurement result, the focus was on finding out the reliability of the sample. Reliability was estimated by average resistance of each cycle. Figure 41 illustrates an example of determining the average resistance of each cycle. Average resistance per cycle of every sample is shown in Figure 42.

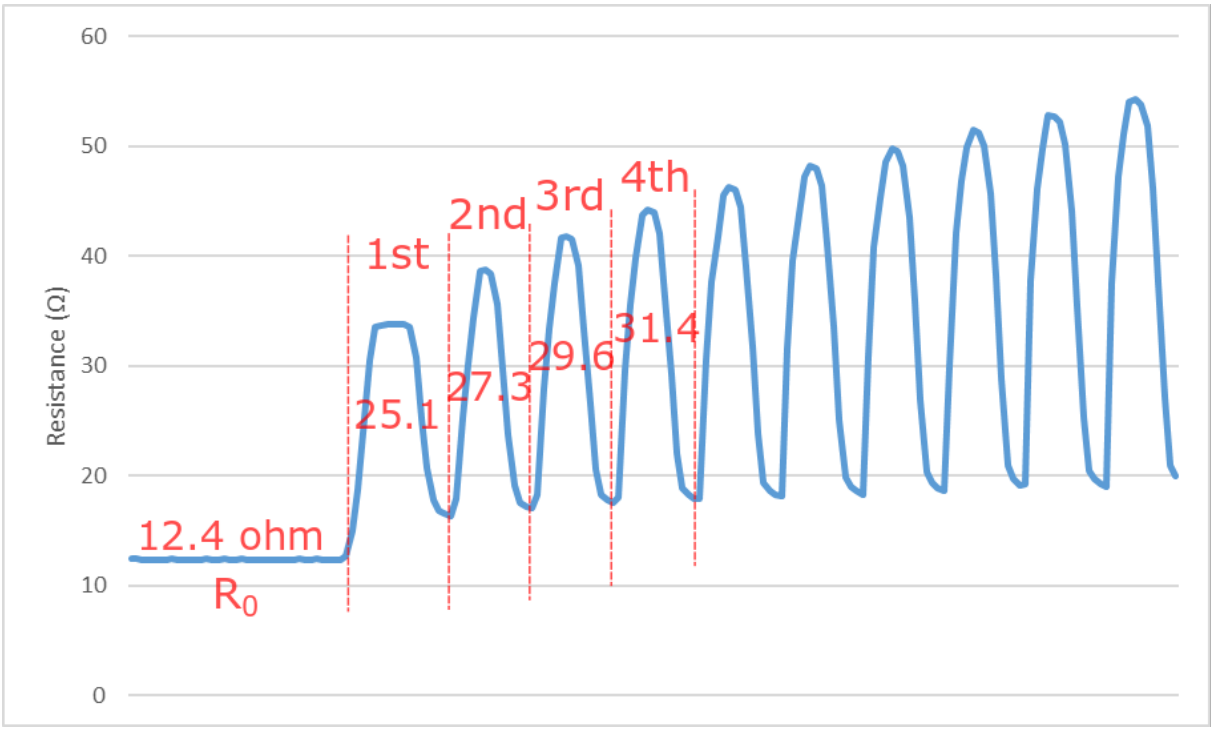

Fig. 41. Example of defined cycles average resistance values.

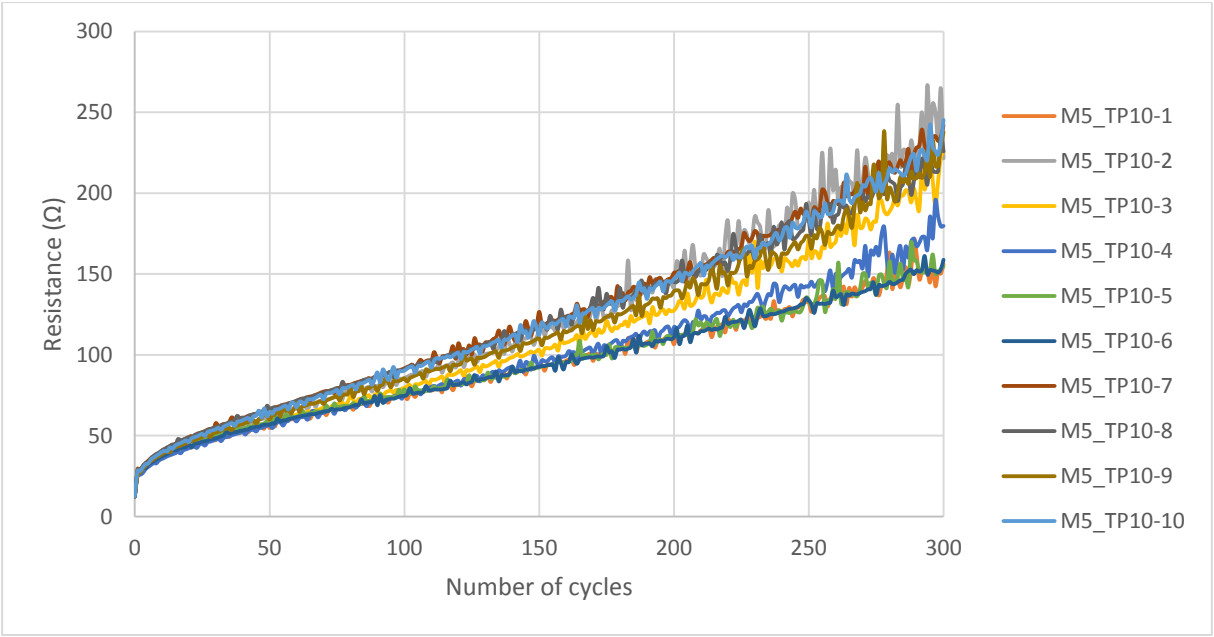

Fig. 42. Average resistance per cycle curve of every sample.

Determining the failure limit to 100 Ω average resistance per cycle, we get useful life of every sample. Failure cycle of samples are presented in Table 14. Weibull distribution was created from Table 14. Scale parameter $\alpha = 1/149$ and the shape parameter $\beta = 6.14$ of Weibull's distribution are obtained by using Weibull Analysis [67]. Measured data and their Weibull distribution are shown in Figure 43. Based on the Weibull distribution of this measurement, it can be assumed that about 91.8 % of the samples have a lifetime of at least

one hundred cycles and 99.8 % of the samples fail before cycle 200, as can be seen in Figure 43.

Table 14. Failure cycle of every sample.

Sample	Cycle
M5_TP10-1	168
M5_TP10-2	121
M5_TP10-3	142
M5_TP10-4	161
M5_TP10-5	164
M5_TP10-6	162
M5_TP10-7	111
M5_TP10-8	117
M5_TP10-9	122
M5_TP10-10	119

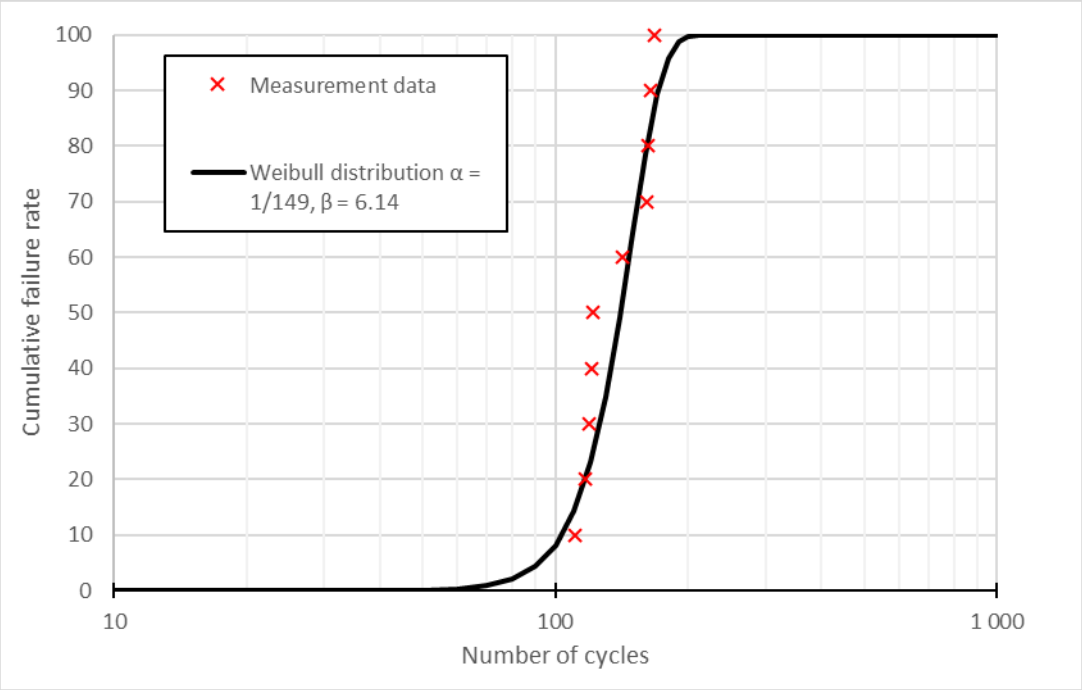

Fig. 43. Cumulative failure rate of samples with Weibull distribution.

5 DISCUSSION

The strain tester device which was implemented in this thesis has a requirement of ± 1% accuracy and load indicator and travel movement at full-scale in ASTM D882-12 standard [51]. Load sensor ± 0.1% at full scale and travel accuracy ± 0.05 mm per 250 mm meets the required accuracy [64, 65]. Also, the resistance meter accuracy between 0.006% and 0.81% can be considered sufficiently accurate [66]. Measuring instruments communicate with a computer that records data from measuring devices and uploads it to a table. The obtained measurement results can be viewed there. The strain tester can be considered successful and suitable for stretching and reliability testing.

The strain tester currently allows only one sample to be tested at the same time. A future development target is to change the resistance meter so that more samples can be connected to same resistance measurement at the same time. In addition, the sample holder should be replaced to allow multiple samples to be attached. In this way, the devices could be subjected to multiple sample tests at the same time and accelerate, in particular, long-term multi-sample cyclic testing. For multi-sample tests, it would not be possible to measure the force applied to every sample.

The aim of the first measurements of this thesis was to compare the effect of printing ink, substrate, drying, wire pattern and screen print direction on elongation. In this evaluation, a stretchability limit test was used, where the sample was stretched until resistance increased over a specific value or failure occurred. Failure type in this case is overstress failure. All the printing ink samples were printed via screen printing and were printed using the same printing net. Substrate thicknesses and drying methods differed between the samples. There were significant differences in the thicknesses of the samples between printing inks; therefore the results cannot be considered as fully comparable. However, on the basis of testing, it was possible to draw conclusions about what samples should be tested further and which deserve more time-consuming cyclic tests, and thereby evaluate the reliability of samples.

The second measurement shows a cyclic stretchability test for one test point. The test samples are made using the roll-to-roll printing technique. In cyclic stretchability tests, usually failures occur as a result of multiple repetitions, i.e. the wear-out failure mechanism. On the basis of the second measurement results, the Weibull distribution could be formed, which can be used to evaluate the wear, duration and reliability of the sample. There were 10 samples tested, so to get a more accurate and reliable result, the number of samples should be increased. In general, a suitable minimum sample size for reliability tests is 30, or according to equation (17).

In cyclic stretchability tests, 100 Ω of average resistance per cycle was used as the limit of failure. Generally in studies, when evaluating the resistance of conductors, a limit of 20% resistance increase is used, but higher values are used when estimating stretchable electronics printed conductors. When stretched, the wire lengthens, resulting in a narrowing and thinning of the conductor, which in itself increases the resistance of the conductor. However, the results of the first and second measurements can be considered very typical in the study of printed stretchable conductors at present.

6 SUMMARY

The aim of this thesis was to implement a stretch tester for printed stretchable electronics conductors on a stretchable substrate, and to test the effect of sample variables and wire patterns affecting different manufacturing and its impact on reliability. At first, the history of stretchable electronics, fabrication techniques and materials were reviewed to inform the current state of stretchable electronics and also fabrication techniques and the properties of materials that affect the durability of the finished sample.

Reliability and testing were investigated in order to be able to evaluate reliability in the right way and sample size. Failure mechanisms for printed conductors on stretchable substrata to know how the samples failures as a result of stretching and what things affect failures of samples. In order to make the strain tester as good as possible with today's research requirements, the standards of stretching electronics testing, as well as other organizations' ways to test stretchable electronics, were also examined.

The strain tester construction was started by adding a resistance meter to the tensile test stand that met requirements. A LabVIEW-based computer program was designed for reading and storing values from the tensile test stand and resistance meter. The sample holders of the tester were coated with rubber in accordance with the standards to avoid damaging the sample.

In the first measurements, the focus was a stretchability limit test for a multiplicity of sample combinations. From these samples, differences were found between printing ink, substrate, drying, wire pattern and screen print direction. The differences between the manufacturers' printing inks were highly variable. The printing inks also have differences between the thicknesses of the conductors, although all were printed with the same printing mesh. A U-shaped wire pattern gave the best results at maximal strain. Also, the horizontal screen print direction was slightly better than vertical.

On the basis of the first measurement, the U-shaped horizontal wire with the thickest 150 µm TPU substrate was selected for the second measurement. The second measurement used printing ink from manufacturer 5, which gave the most steady results in the first measurement. Ten similar samples were subjected to a cyclic stretchability limit test to assess samples' reliability. The reliability comparison was made on the basis of average resistance per cycle. The failure limit was determined to be 100 Ω average resistance per cycle. Based on the duration of the samples, Weibull's distribution was formed, which was used to estimate the life of the sample.

7 REFERENCES

[1] Rogers J. A., Someya T., Huang Y. (2010) Materials and mechanics for stretchable electronics. Science, vol. 327, pp. 1603-1607. DOI: 10.1126/science.1182383

[2] VTT Technical Research Centre of Finland (2018) Stretchable electronics to boost Finnish export industry URL: https://www.vttresearch.com/media/news/stretchable-electronics-to-boost-finnish-export-industry , Cited 26.10.2018

[3] Ahn J-H., Je J. H (2012) Stretchable electronics: Materials, architectures and integrations. Journal of Physics D Applied Physics, Vol 45, Issue 10 DOI: 10.1088/0022-3727/45/10/103001

[4] Ghaffarzadeh K. (2017) Stretchable electronics: everything you need to know URL: https://www.idtechex.com/research/articles/stretchable-electronics-everything-you-need-to-know-00010988.asp , Cited 25.10.2018

[5] Jang K-I., Li K., Chung H. U. Xu S., Jung H. N., Yang Y., Kwak J. W., Jung H. H., Song J., Yang C., Wang A., Liu Z., Lee J. Y., Kim B. H., Kim J-H., Lee J., Yu Y., Kim B. J., Jang H., Yu K. J., Kim J., Lee J. W., Jeong J-W., Song Y. M., Huang Y., Zhang Y., Rogers J. A (2017) Self-assembled three dimensional network designs for soft electronics. Nature Communications, Vol 8, Article number: 15894 DOI: 10.1038/ncomms15894

[6] Ma Y., Feng X., Rogers J. A., Huang Y., Zhang Y. (2017) Design and application of 'J-shaped' stress–strain behavior in stretchable electronics: a review. Lab on a Chip, Vol 17, Issue 10, pp. 1689-1704. DOI: 10.1039/C7LC00289K

[7] Aleeva, Y., Pignataro B. (2014) Recent advances in upscalable wet methods and ink formulations for printed electronics. Journal of Materials Chemistry C, Vol 2, Issue 32, pp. 6436-6453. DOI: 10.1039/c4tc00618f

[8] Laing J., Tong K., Pei Q. (2016) A Water-Based Silver-Nanowire Screen-Print Ink for the Fabrication of Stretchable Conductors and Wearable Thin-Film Transistors. Advanced Materials, Vol 30, Issue 28, pp. 5986-5996. DOI: 10.1002/adma.201600772

[9] Jianhui L., Bing Y., Xiaoming W., Tianling R., Litian L. (2009) Stretchable Interconnections for Flexible Electronic Systems. In: 31st Annual International Conference of the IEEE EMBS, September 2-6, Minneapolis, Minnesota, USA, pp. 4124-4127. DOI: 10.1109/IEMBS.2009.5332697

[10] Takei K. (2018) History of Flexible and Stretchable Devices. Wiley-VCH DOI: 10.1002/9783527804856.ch1

[11] Beck J. (2011) Archive Gallery: The Telephone. URL: https://www.popsci.com/gadgets/article/2011-10/archive-gallery-improving-telephone , Cited 30.10.2018

[12] Hammock M. L., Chortos A., Tee B. C.-K., Tok T. B.-H., Bao Z. (2013) 25th Anniversary Article: The Evolution of Electronic Skin (E-Skin): A Brief History, Design Considerations, and Recent Progress. Advanced Materials, Vol 25, Issue 42, pp. 5997-6038. DOI: 10.1002/adma.201302240

[13] Garnier, F., Horowitz, G., Peng, X., and Fichou, D. (1990) An all- organic "soft" thin film transistor with very high carrier mobility. Advanced Materials, Vol 2, Issue 12, pp. 592-594. DOI: 10.1002/adma.19900021207

[14] Gustafsson, G., Cao, Y., Treacy, G.M., Klavetter, F., Colaneri, N., and Heeger, A.J. (1992) Flexible light-emitting diodes made from soluble conducting polymers. Nature, Vol 357, pp. 477-479. DOI: 10.1038/357477a0

[15] Gray D. S., Tien J., Chen C. S. (2004) High-Conductivity Elastomeric Electronics. Advanced Materials, Vol 16, Issue 5 pp. 393-397. DOI: 10.1002/adma.200306107

[16] Li T., Huang Z., Suo Z., Lacour S. P., Wagner S. (2004) Stretchability of thin metal films on elastomer substrates. Applied Physics Letters, Vol 85, Issue 16 DOI: 10.1063/1.1806275

[17] Lacour S. P., Jones S., Suo Z., Wagner S. (2004) Design and Performance of Thin Metal Film Interconnects for Skin-Like Electronic Circuits. IEEE Electron Device Letter, Vol 25, Issue 4, pp 179-181 DOI: 10.1109/LED.2004.825190

[18] Löher T., Manessis D, Heinrich R., Schmied B., Vanfleteren J., DeBaets J., Ostmann A., Reichl H. (2006) Stretchable electronic systems. In: Electronics Packaging Technology Conference. December 6 - 8, Singapore, pp. 271-276 DOI: 10.1109/EPTC.2006.342728

[19] Song Z., Ma T., Cheng Q., Wang X., Krishnaraju D., panat R., Chan C. K., Yo H., Jiang h. (2014) Origami lithium-ion batteries. Nature Communications, Vol 5, Article number: 3140 DOI: 10.1038/ncomms4140

[20] Xu S., Zhang Y., Cho J., Lee J., Huang X., Jia L., Fan J. A., Su Y., Su J., Zhang H., Cheng H., Lu B., Yu C., Chuang C., Kim T., Song T., Shigeta K., Kang S., Dagdeviren C., Petrov I., Braun P. V., Huang Y., Paik U., Rogers J. A. (2013) Stretchable batteries with self-similar serpentine interconnects and integrated wireless recharging systems, Nature Communications, Vol 4, Article number: 1543 DOI: 10.1038/ncomms2553

[21] Kim D-H., Lu N., Ma R., Kim Y-S., Kim R-H, Wang S., Wu J., Won S. M., Tao H., Islam A., Yu K. J., Kim T., Chowdhury R., Ying M., Xu L., Li M., Chung H-J., Keum H., McCormick M., Liu P., Zhang Y-W., Omenetto F. G., Huang Y., Coleman T., Rogers J. A. (2011) Epidermal Electronics. Science, Vol 333, Issue 6044, pp. 838-843. DOI: 10.1126/science.1206157

[22] Amjadi M., Pichitpajongkit A, Lee S, Ryu S., Park I. (2014) Highly Stretchable and Sensitive Strain Sensor Based on Silver Nanowire–Elastomer Nanocomposite. ACS Nano, Vol 8, Issue 5, pp. 5154-5163. DOI: 10.1021/nn501204t

[23] Myontec URL: https://www.myontec.com/products/mbody/ , Cited 6.11.2018

[24] Liu Y., Pharr M., Salvatore G. A. (2017) Lab-on-Skin: A Review of Flexible and Stretchable Electronics for Wearable Health Monitoring. ACS Nano, Vol 11, Issue 10, pp. 9614-9635. DOI: 10.1021/acsnano.7b04898

[25] Nisato, G., Lupo, D., Ganz, S. (2016) Organic and printed electronics: Fundamentals and applications. Singapore, Pan Stanford Publishing

[26] Hannila E. (2018) Testijärjestelmän kehittäminen painettavan elektroniikan luotettavuustestaukseen. Diplomityö, Oulun yliopisto, Tieto- ja sähkötekniikan tiedekunta, Oulu.

[27] Kipphan H. (2001) Handbook of Print Media Technologies and Production Methods. Springer, Germany. DOI: 10.1007/978-3-540-29900-4

[28] Abbott S. (2008) How to be a great screen printer. Macdermid Autotype Limited.

[29] Søndergaard R, Hösel M, Angmo D, Larsen-Olsen TT & Krebs FC (2012) Roll-to-roll fabrication of polymer solar cells. Materials Today, Vol 15, Number 1–2, pp. 36–49. DOI: 10.1016/S1369-7021(12)70019-6

[30] Mohammed A., Pecht M. (2016) A stretchable and screen-printable conductive ink for stretchable electronics. Applied Physics Letters, Vol 109, Issue 18 DOI: 10.1063/1.4965706

[31] Nelo M. (2015) Inks based on inorganic nanomaterials for printed electronics applications. Doctoral thesis, University of Oulu, Faculty of Information Technology and Electrical Engineering, Department of Electrical Engineering

[32] Happonen, Tuomas (2016) Reliability studies on printed conductors on flexible substrates under cyclic bending. Doctoral thesis, University of Oulu, Faculty of Information Technology and Electrical Engineering

[33] Levin M. A., Kalal T. T. (2003) Improving Product Reliability. West Sussex, England, John Wiley & Sons Ltd.

[34] Mishra, R. & Sandilya, A. (2009) Reliability and Quality Management.

[35] Barlow R. E., Proschan F. (1975) Statistical Theory of Reliability and Life Testing Probability Models. Holt, Rinehart and Winston Inc, New York, 290 pp.

[36] Happonen T., Voutilainen J-H., Häkkinen J., Fabritius T. (2016) The Effect of Width and Thickness on Cyclic Bending Reliability of Screen-Printed Silver Traces on a Plastic Substrate. IEEE Transactions on Components, Packaging and Manufacturing Technology, Vol 6, Issue 5 DOI: 10.1109/TCPMT.2016.2544441

[37] Yang G. (2009) Reliability Demonstration Through Degradation Bogey Testing. IEEE Transactions on Reliability, Vol 58, Issue 4, pp. 604-610 DOI: 10.1109/TR.2009.2033733

[38] Sullivan L., LaMorte W. Confidence Intervals for a Single Mean or Proportion. Boston University School of Public Health URL: http://sphweb.bumc.bu.edu/otlt/MPH-Modules/QuantCore/PH717_ConfidenceIntervals-OneSample/PH717_ConfidenceIntervals-OneSample_print.html , Cited 21.02.2019

[39] Pecht M., Gu J (2009) Physics-of-failure-based prognostics for electronic products. Transactions of the Institute of Measurement and Control, Vol 31, Issue 3-4, pp. 309-322 DOI: 10.1177/0142331208092031

[40] Dai L., Huand Y., Chen H., Feng Z., Fang D (2015) Transition among failure modes of the bending system with a stiff film on a soft substrate. Appl Phys Lett, Vol 106, Issue 2 DOI: 10.1063/1.4905697

[41] Kim K-S., Jung K-H., Jung S-B. (2014) Design and fabrication of screen-printed silver circuits for stretchable electronics. Microelectronic Engineering, Vol 120, pp. 216-220 DOI: 10.1016/j.mee.2013.07.003

[42] Qi J. (2000) Measurement of Surface and Interfacial Energies between Solid Materials Using an Elastica Loop. Master thesis, Virginia Polytechnic Institute and State University.

[43] Maugis D., Pollock H. M. (1984) Surface forces, deformation and adherence at metal microcontacts. Acta metal, Vol. 32, Number 9, pp. 1323-1334

[44] Bruce R. B. (2012) Handbook of Lubrication and Tribology, Volume II: Theory and Design, Second Edition. CRC Press, ISBN 9781420069082

[45] Park S-I., Ahn J-H., Feng X., Wang S., Huang Y., Rogers J. A. (2018) Theoretical and Experimental Studies of Bending of Inorganic Electronic Materials on Plastic Substrates. Advanced Functional Materials, Vol. 18, Issue 18, pp. 2673-2684 DOI: 10.1002/adfm.200800306

[46] Merilampi S., Laine-Ma T., Ruuskanen P. (2009) The characterization of electrically conductive silver ink patternson flexible substrates. Microelectronics Reliability, Vol 49, Issue 7, pp. 782-790 DOI: 10.1016/j.microrel.2009.04.004

[47] Merilampi S., Björninen T., Haukka V., Ruuskanen P., Ukkonen L., Sydänheimo L. (2010) Analysis of electrically conductive silver ink on stretchable substrates under tensile load. Microelectronics Reliability, Vol 50, Issue 12, pp. 2001-2011 DOI: 10.1016/j.microrel.2010.06.011

[48] Suomen Standardisoimisliitto SFS ry (2017) Vuosikertomus 2017

[49] ISO International Organization for Standardization (2017) ISO 216:2007: Writing paper and certain classes of printed matter -- Trimmed sizes -- A and B series, and indication of machine direction.

[50] IPC Electronics. (2017) IPC-9204: Guideline on Flexibility and Stretchability Testing for Printed Electronics

[51] ASTM International. (2017). D882-12: Standard Test Method for Tensile Properties of Thin Plastic Sheeting.

[52] Wang L (2010) Mechanical Characterization of Flexible and Stretchable Electronic Substrates. Doctoral thesis, Guilin University of Electronic Technology, China

[53] Lee H., Seong B., Moon H., Byun D (2015) Directly printed stretchable strain sensor based on ring and diamond shaped silver nanowire electrodes. RSC Advances, Vol 5, Issue 36, pp. 28379-28384 DOI: 10.1039/c5ra01519g

[54] Suikkola J (2015) Printed Stretchable Interconnects for Wearable Health and Wellbeing Applications. Master Thesis, Tampere University of Technology, Faculty of Computing and Electrical Engineering, Tampere

[55] Mosallaei M., Khorramdel B., Honkanen M., Iso-Ketola P., Vanhala J, Mäntysalo M (2017) Fabrication and Characterization of Screen Printed Stretchable Carbon Interconnects. In: 2017 IMAPS Nordic Conference on Microelectronics Packaging (NordPac), June 18-20, Gothenburg, Sweden DOI: 10.1109/NORDPAC.2017.7993169

[56] Suikkola J., Björninen T., Mosallaei M., Kankkunen T., Iso-Ketola P., Ukkonen L., Vanhala J., Mäntysalo M. (2015) Screen-Printing Fabrication and Characterization of Stretchable Electronics. Scientific Reports, Vol 6, Article number: 25784 DOI: 10.1038/srep25784

[57] Kim C., Kim C. H. (2018) Universal Testing Apparatus Implementing Various Repetitive Mechanical Deformations to Evaluate the Reliability of Flexible Electronic Devices. Micromachines, Vol: 9, Issue: 10 DOI: 10.3390/mi9100492

[58] Bossuyt F., Guenther J., Löher T., Seckel M., Sterken T., de Vries J. (2012) Cyclic endurance reliability of stretchable electronic substrates. Microelectronics Reliability, Vol 51, Issue 3, pp. 628-635 DOI: 10.1016/j.microrel.2010.09.032

[59] Park J. J., Hyun W. J., Mun S. C., Park Y. T., Park O. O (2015) Highly Stretchable and Wearable Graphene Strain Sensors with Controllable Sensitivity for Human Motion Monitoring. ACS Appl. Mater. Interfaces, Vol 7, Issue 11, pp. 6317-6324 DOI: 10.1021/acsami.5b00695

[60] Fan X., Wang N., Yan F., Wang J., Song W., Ge Z. (2018) A Transfer- Printed, Stretchable, and Reliable Strain Sensor Using PEDOT:PSS/Ag NW Hybrid Films Embedded into Elastomers. Adv. Mater. Technol. Vol 3, Issue 6 DOI: 10.1002/admt.201800030

[61] Byun J., Lee B., Oh E., Kim H., Kim S., Lee S., Hong Y. (2017) Fully printable, strain-engineered electronic wrap for customizable soft electronics. Scientific Reports, Vol 7, Article number: 45328 DOI: 10.1038/srep45328

[62] Eptanova (2018) Stretchable electronics. URL: https://www.eptanova.com/en/news/stretchable-electronics , Cited 23.01.2019

[63] Hocheng H., Chen C-M. (2014) Design, Fabrication and Failure Analysis of Stretchable Electrical Routings. Sensors, Vol 14, Issue 7, pp. 11855-11877 DOI: 10.3390/s140711855

[64] Mark-10 Corporation. Models ESM303 & ESM303H FORCE TEST STANDS User's Guide URL: http://www.mark-10.com/new_manuals/manualESM303.pdf , Cited 28.01.2019

[65] Mark-10 Corporation. Series 7 DIGITAL FORCE GAUGES User's Guide URL: http://www.mark-10.com/new_manuals/manualSeries7.pdf , Cited 29.01.2019

[66] Hewlett-Packard Company (1996) HP 34401A Multimeter User's Guide

[67] Dorner W. (2019) Using Microsoft Excel for Weibull Analysis. Quality Digest. URL: https://www.qualitydigest.com/magazine/1999/jan/article/using-microsoft-excel-weibull-analysis.html , Cited 12.03.2019

8 APPENDICES

Appendix 1 Example of strain test results.

Appendix 2 Resistance-strain graph of samples.

Appendix 3 Max strain of samples.

Appendix 4 Initial resistance of samples.

Appendix 1 Example of strain test result text file.

Time	Travel	Force	Resistance	Overload
0,000	0,0000	-0,0400	2,8518	0
1,105	0,0000	-0,0400	2,8379	0
1,299	0,0000	-0,0400	2,8101	0
1,493	0,0000	-0,0400	2,8518	0
1,687	0,0000	-0,0400	2,8657	0
1,881	0,0000	-0,0400	2,7892	0
2,076	0,0000	-0,0400	2,7962	0
2,269	0,0000	-0,0400	2,8657	0
2,463	0,0000	-0,0400	2,8310	0
2,658	0,0000	-0,0400	2,7823	0
2,852	0,0000	-0,0400	2,8796	0
3,046	0,0000	-0,0400	2,8588	0
3,240	0,0000	-0,0400	2,7823	0
3,433	0,0000	-0,0400	2,8518	0
3,626	0,0000	-0,0400	2,8657	0
3,821	0,0000	-0,0400	2,7892	0
4,015	0,0000	-0,0400	2,7823	0
4,210	0,0000	-0,0400	2,8796	0
4,404	0,0400	-0,0200	2,9214	0
4,599	0,6200	0,5400	3,0048	0
4,793	1,1800	0,9600	3,2831	0
4,987	1,7600	1,3500	3,7422	0
5,181	2,3600	1,7200	4,2290	0
5,375	2,9400	2,0300	5,0081	0
5,569	3,5200	2,3400	5,9262	0
5,762	4,1000	2,6500	6,8514	0
5,957	4,6800	2,9300	7,8321	0
6,151	5,2800	3,2000	8,9798	0
6,344	5,8600	3,4800	10,1483	0
6,539	6,4400	3,7400	11,2752	0
6,733	7,0200	3,9600	12,5272	0
6,926	7,5800	4,2000	13,8488	0
7,120	8,1600	4,4300	15,1495	0
7,315	8,7800	4,6300	16,6241	0
7,510	9,3400	4,8000	18,1682	0
7,704	9,9200	5,0000	19,7750	0
7,899	10,5000	5,1800	21,3470	0
8,093	11,0800	5,3600	23,0581	0
8,286	11,6800	5,5100	24,8805	0
8,481	12,2600	5,6700	26,6263	0
8,675	12,8400	5,8400	28,5739	0
8,869	13,4200	5,9700	30,4242	0
9,064	14,0200	6,1000	32,1700	0
9,257	14,6000	6,2500	34,1733	0
9,452	15,1800	6,3800	36,1765	0

9,648	15,7600	6,5000	38,4928	0
9,842	16,3400	6,6200	40,5795	0
10,035	16,9400	6,7300	42,7844	0
10,230	17,5000	6,8500	45,0937	0
10,423	18,0800	6,9600	47,3891	0
10,619	18,6800	7,0600	49,6358	0
10,813	19,2400	7,1400	51,7642	0
11,006	19,8200	7,2500	56,0976	0
11,202	20,4400	7,3600	61,0013	0
11,396	21,0000	7,4300	82,4874	0
11,589	21,5800	7,5100	69,5777	0
11,783	22,1600	7,6200	71,9844	0
11,977	22,7400	7,6800	89,2414	0
12,170	23,3400	7,7500	101,4973	0
12,365	23,9200	7,8400	106,6793	0
12,560	24,5000	7,9300	1500,0000	1
12,753	25,0800	7,9800	1500,0000	1
12,947	25,6600	8,0600	183,3379	0
13,142	26,2600	8,1300	1500,0000	1
13,336	26,8400	8,2000	1500,0000	1
13,530	27,4000	8,2500	1500,0000	1
13,724	27,9800	8,3200	1500,0000	1
13,918	28,3600	8,3100	1500,0000	1
14,112	28,3600	8,1400	1500,0000	1
14,306	28,3600	8,0300	1500,0000	1
14,499	28,3600	7,9400	1500,0000	1
14,694	28,3600	7,8700	1500,0000	1
14,888	28,3600	7,8200	1500,0000	1
15,082	28,3600	7,7700	1500,0000	1
15,276	28,3600	7,7200	1500,0000	1
15,470	28,3600	7,6800	1500,0000	1
15,664	28,3600	7,6500	1500,0000	1
15,858	28,3600	7,6100	1500,0000	1
16,052	28,3600	7,5900	1500,0000	1
16,246	28,3600	7,5600	1500,0000	1
16,440	28,3600	7,5300	1500,0000	1
16,634	28,3600	7,5100	1500,0000	1
16,828	28,3600	7,4900	1500,0000	1
17,022	28,3600	7,4600	1500,0000	1
17,216	28,3600	7,4400	1500,0000	1
17,410	28,3600	7,4300	1500,0000	1

Appendix 2 Resistance-strain graph of samples.

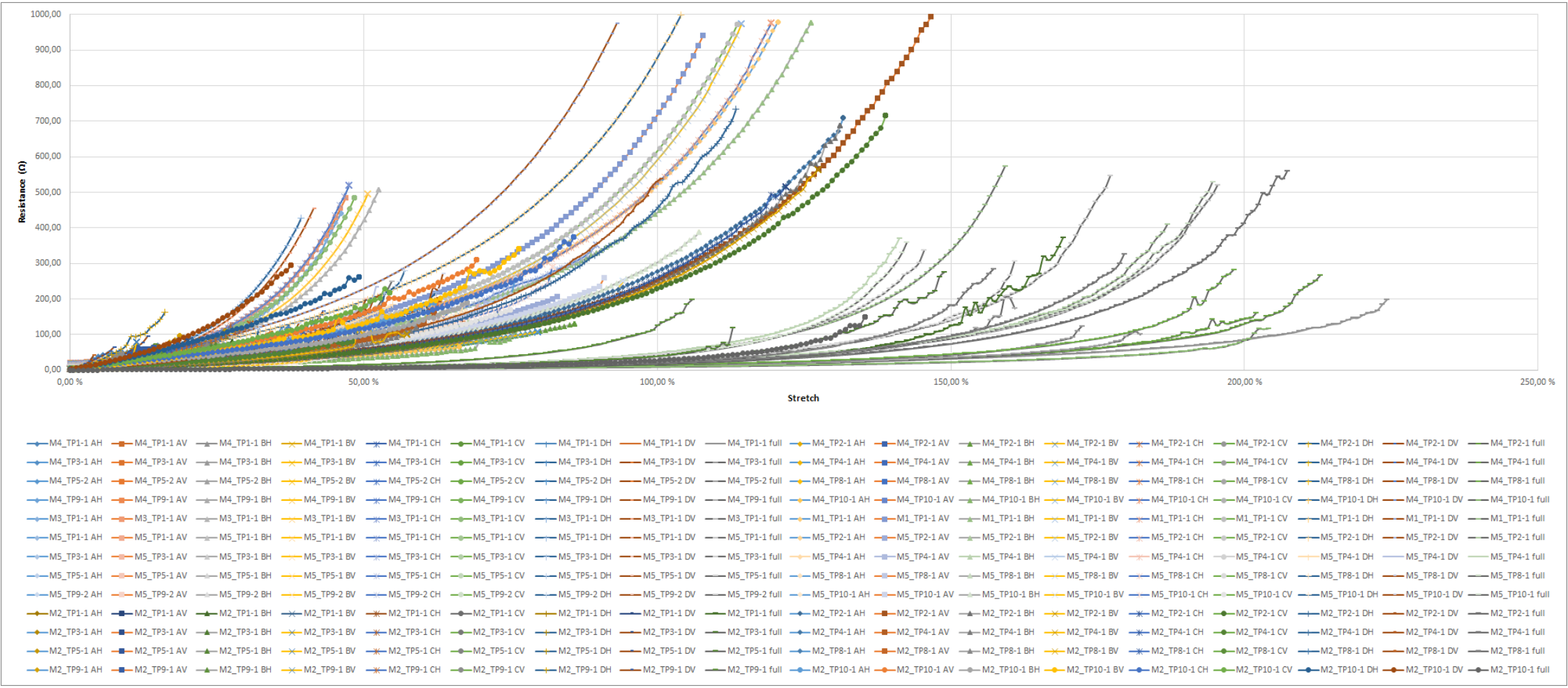

Appendix 3 Max strain of samples.

	M4_TP1-1	M4_TP2-1	M4_TP3-1	M4_TP4-1	M4_TP5-2	M4_TP8-1	M4_TP9-1	M4_TP10-1	M3_TP1-1	M1_TP1-1	M5_TP1-1	M5_TP2-1	M5_TP3-1
AH	37,14 %	50,57 %	37,17 %	63,09 %	23,06 %	59,74 %	15,11 %	66,31 %	46,11 %	120,51 %	59,74 %	59,63 %	14,06 %
AV	66,89 %	81,37 %	52,06 %	42,57 %	20,66 %	30,83 %	15,49 %	29,97 %	46,94 %	107,80 %	79,17 %	83,00 %	51,94 %
BH	51,00 %	85,91 %	45,83 %	51,17 %	26,00 %	39,00 %	14,31 %	75,69 %	52,60 %	126,20 %	51,57 %	46,00 %	63,06 %
BV	74,91 %	79,57 %	41,89 %	79,57 %	22,46 %	40,26 %	18,57 %	45,83 %	50,69 %	114,37 %	50,57 %	73,26 %	60,69 %
CH	74,69 %	41,20 %	37,80 %	42,43 %	22,91 %	49,89 %	11,60 %	42,89 %	47,51 %	119,43 %	78,43 %	69,40 %	89,66 %
CV	64,66 %	48,14 %	29,26 %	18,97 %	24,83 %	30,46 %	10,71 %	30,60 %	48,40 %	113,66 %	44,29 %	57,43 %	57,49 %
DH	36,91 %	24,54 %	23,57 %	49,20 %	19,86 %	42,29 %	2,86 %	23,80 %	39,34 %	104,03 %	62,23 %	41,40 %	35,66 %
DV	34,17 %	29,40 %	20,23 %	16,14 %	17,40 %	43,06 %	6,49 %	27,29 %	41,46 %	93,06 %	43,29 %	50,23 %	48,26 %
full	224,26 %	212,89 %	172,34 %	202,00 %	182,26 %	198,14 %	160,89 %	204,14 %	54,77 %	159,20 %	195,43 %	186,89 %	177,14 %
AVG	73,85 %	72,62 %	51,13 %	62,79 %	39,94 %	59,30 %	28,45 %	60,72 %	47,54 %	117,58 %	73,86 %	74,14 %	66,44 %
	M5_TP4-1	M5_TP5-1	M5_TP8-1	M5_TP9-2	M5_TP10-1	M2_TP1-1	M2_TP2-1	M2_TP3-1	M2_TP4-1	M2_TP5-1	M2_TP8-1	M2_TP9-1	M2_TP10-1
AH	66,94 %	75,86 %	51,94 %	42,94 %	67,40 %	22,09 %	131,66 %	23,74 %	58,23 %	26,40 %	17,49 %	18,69 %	61,97 %
AV	70,89 %	52,83 %	46,77 %	37,11 %	90,91 %	11,26 %	146,63 %	7,89 %	62,83 %	21,06 %	16,69 %	14,26 %	69,29 %
BH	67,83 %	56,80 %	46,91 %	54,20 %	107,17 %	27,57 %	131,11 %	31,49 %	58,89 %	26,49 %	23,40 %	15,91 %	67,66 %
BV	57,54 %	51,43 %	37,51 %	43,14 %	94,14 %	20,17 %	127,34 %	24,06 %	57,40 %	25,06 %	14,60 %	11,31 %	76,40 %
CH	53,00 %	54,91 %	50,31 %	37,60 %	82,11 %	19,80 %	121,86 %	12,17 %	48,80 %	30,69 %	18,09 %	8,34 %	85,83 %
CV	45,43 %	37,23 %	44,69 %	27,63 %	75,00 %	12,86 %	138,91 %	18,11 %	48,06 %	11,46 %	14,54 %	8,74 %	54,40 %
DH	54,91 %	56,94 %	34,23 %	32,17 %	62,26 %	11,97 %	113,43 %	11,26 %	40,51 %	11,43 %	8,89 %	16,17 %	49,23 %
DV	52,09 %	50,34 %	38,89 %	23,14 %	63,46 %	13,26 %	100,60 %	19,77 %	52,51 %	13,17 %	4,00 %	7,43 %	37,66 %
full	141,20 %	145,43 %	194,54 %	160,83 %	142,51 %	169,11 %	207,29 %	148,91 %	179,49 %	112,86 %	157,29 %	105,91 %	135,34 %
AVG	67,76 %	64,64 %	60,64 %	50,97 %	87,22 %	34,23 %	135,43 %	33,04 %	67,41 %	30,96 %	30,55 %	22,97 %	70,86 %

Appendix 4 Initial resistance of samples.

	M4_TP1-1	M4_TP2-1	M4_TP3-1	M4_TP4-1	M4_TP5-2	M4_TP8-1	M4_TP9-1	M4_TP10-1	M3_TP1-1	M1_TP1-1	M5_TP1-1	M5_TP2-1	M5_TP3-1
AH	5,98	5,50	5,22	5,54	4,25	6,24	3,41	4,08	18,52	14,73	7,07	7,34	8,10
AV	6,08	5,57	5,35	5,46	4,17	5,72	3,39	4,09	20,75	16,82	7,25	7,81	7,85
BH	5,73	5,28	4,87	5,27	4,08	6,16	3,22	3,91	18,22	13,78	6,57	6,98	7,38
BV	5,78	5,20	4,81	5,20	4,00	5,37	3,22	3,91	19,41	15,31	6,86	7,34	7,18
CH	6,01	5,53	5,19	5,46	4,34	6,28	3,46	4,06	20,19	14,85	7,09	7,63	7,87
CV	5,83	5,29	5,04	5,51	4,13	5,34	3,27	4,08	19,28	15,25	7,03	7,45	7,37
DH	3,11	2,60	2,50	2,53	2,03	2,93	1,63	1,86	11,54	8,41	3,68	3,98	0,00
DV	2,83	2,54	2,47	2,44	1,99	2,78	1,53	1,87	9,31	8,48	3,32	3,76	3,83
full	0,26	0,14	0,15	0,16	0,12	0,15	0,10	0,12	0,61	0,46	0,20	0,21	0,22
AVG	4,62	4,18	3,95	4,17	3,23	4,55	2,58	3,11	15,31	12,01	5,45	5,83	5,53
	M5_TP4-1	M5_TP5-1	M5_TP8-1	M5_TP9-2	M5_TP10-1	M2_TP1-1	M2_TP2-1	M2_TP3-1	M2_TP4-1	M2_TP5-1	M2_TP8-1	M2_TP9-1	M2_TP10-1
AH	8,02	8,04	8,05	6,29	8,37	4,38	5,05	4,46	5,13	4,83	4,44	4,63	5,89
AV	7,81	7,80	7,62	5,89	7,81	4,28	4,72	4,43	4,64	4,66	4,67	4,73	5,23
BH	7,49	7,52	7,36	5,89	7,61	4,20	4,68	4,30	4,37	4,88	4,41	4,37	5,26
BV	7,43	7,37	7,07	5,66	7,72	4,18	4,34	4,30	4,56	4,44	4,37	4,56	5,23
CH	8,02	8,10	7,72	6,20	8,07	4,46	5,04	4,56	4,88	4,85	4,61	4,62	5,74
CV	7,65	7,75	7,21	5,94	8,02	4,40	4,55	4,60	5,03	4,65	4,61	4,65	5,13
DH	4,00	4,05	4,14	2,95	3,92	2,17	3,20	2,18	2,68	2,31	2,33	2,13	3,58
DV	3,77	3,80	3,60	2,93	3,64	1,88	2,37	2,09	2,16	2,24	2,08	2,25	2,56
full	0,24	0,23	0,22	0,18	0,23	0,10	0,11	0,09	0,12	0,11	0,09	0,12	0,11
AVG	6,05	6,07	5,89	4,66	6,15	3,34	3,78	3,44	3,73	3,66	3,51	3,56	4,30